



**HAL**  
open science

## The depositional record of the French Flemish Coastal plain since antiquity: Impacts of land reclamation in a tide-dominated estuary

Rachid Ouchaou, Jean-yves Reynaud, Youn Besse, Anissa Tilehghouatine, Eric Armynot Du Châtelet, Alain Trentesaux, Romain Abraham, Laurent Deschodt, Guillaume Hulin, Samuel Desoutter, et al.

### ► To cite this version:

Rachid Ouchaou, Jean-yves Reynaud, Youn Besse, Anissa Tilehghouatine, Eric Armynot Du Châtelet, et al.. The depositional record of the French Flemish Coastal plain since antiquity: Impacts of land reclamation in a tide-dominated estuary. *Depositional Record*, 2024, 10.1002/dep2.279 . hal-04583376

**HAL Id: hal-04583376**

**<https://hal.science/hal-04583376>**

Submitted on 23 May 2024


**HAL** is a multi-disciplinary open access archive for the deposit and dissemination of scientific research documents, whether they are published or not. The documents may come from teaching and research institutions in France or abroad, or from public or private research centers.

L'archive ouverte pluridisciplinaire **HAL**, est destinée au dépôt et à la diffusion de documents scientifiques de niveau recherche, publiés ou non, émanant des établissements d'enseignement et de recherche français ou étrangers, des laboratoires publics ou privés.



Distributed under a Creative Commons Attribution 4.0 International License

# The depositional record of the French Flemish Coastal plain since antiquity: Impacts of land reclamation in a tide-dominated estuary

Rachid Ouchaou<sup>1</sup> | Jean-Yves Reynaud<sup>1</sup>  | Youn Besse<sup>1</sup> | Anissa Tilehghouatine<sup>1</sup> | Eric Armynot du Châtelet<sup>1</sup> | Alain Trentesaux<sup>1</sup> | Romain Abraham<sup>1</sup> | Laurent Deschodt<sup>2,3</sup> | Guillaume Hulin<sup>2,4</sup> | Samuel Desoutter<sup>2,5</sup> | Benjamin Fores<sup>2,4</sup> | François-Xavier Simon<sup>2,6</sup> | Mathieu Lançon<sup>2,4</sup>

<sup>1</sup>LOG UMR 8187—

CNRS|ULille|ULCO|IRD, Université de Lille, Lille, France

<sup>2</sup>INRAP, Institut National de Recherches Archéologiques Préventives, Paris, France

<sup>3</sup>UMR 8591 LGP, Université de Créteil, Créteil, France

<sup>4</sup>UMR 7619 METIS, CNRS, Sorbonne Université, Paris, France

<sup>5</sup>UMR 8593 IRHiS, Université de Lille, Lille, France

<sup>6</sup>UMR 6249 LCE, CNRS, Université de Franche-Comté, Besançon, France

## Correspondence

Jean-Yves Reynaud, LOG UMR 8187—CNRS|ULille|ULCO|IRD, Université de Lille, Lille, France.

Email: [jean-yves.reynaud@univ-lille.fr](mailto:jean-yves.reynaud@univ-lille.fr)

## Funding information

SFR Campus de la Mer

## Abstract

The French Flemish Coastal Plain, which extends from Denmark to France, is characterised by a topography close to sea level and protected by a system of coastal dunes. Quaternary sediments, comprised of marine, estuarine and continental deposits, accumulated by infilling and then prograding above a network of incised valleys. This study focusses on the Holocene infill of the Denna palaeoestuary, south-west to Dunkerque. Surface geophysics (electrical conductivity and ground-penetrating radar) and vibrocore data are used to reconstruct the landscape evolution during the last stages of sedimentation. The conductivity map highlights the last network of tidal channels, ditches and dikes of the eastern side of the palaeoestuary. Over the upper 4 m of the infill, the ground-penetrating radar profiles show two superimposed units. The bottom unit is composed of meandering channel bars and the top unit of flat strata intersected by sparse channels, mostly infilled in place. The sediment analysis of the vibrocores shows a predominantly sandy filling of marine to estuarine origin, evidenced by sponge spicules and a fauna of bivalves and foraminifera adapted to brackish settings. The uppermost deposit exhibits an oxidation profile which marks the groundwater zone transition. Clayey sediments are also present, infilling the uppermost channels and ditches dug during reclamation, in increasing proportions towards the axis of the estuarine palaeovalley. The tidal signature of sedimentary dynamics is evidenced by heterolithic facies in some channel fills and tidal rhythmites infilling scour depressions linked to dike breaching. The abrupt decrease in channel dynamics across the unit boundary, although sedimentation remained sandy in the upper unit, coincides with the development of embankment of the estuarine border and is tentatively interpreted as a result of reclamation.

This is an open access article under the terms of the [Creative Commons Attribution](https://creativecommons.org/licenses/by/4.0/) License, which permits use, distribution and reproduction in any medium, provided the original work is properly cited.

© 2024 The Authors. *The Depositional Record* published by John Wiley & Sons Ltd on behalf of International Association of Sedimentologists.

**KEYWORDS**

dike breaching, Flemish plain, France, geoarchaeology, ground-penetrating radar, Holocene, North Sea, reclamation, tidal rhythmites, vibrocores

## 1 | INTRODUCTION

Nearly 50% of the world's population lives in coastal plains, low coastal areas filled with recent deltaic or estuarine sediments (McMichael et al., 2020). Climate change and pressure on water resources in the near sub-surface make detailed knowledge of these spaces a major challenge for development (Dynesius & Nilsson, 1994; Mastroicco & Colombani, 2021). The fine topographic evolution, in particular, reflects either a subsidence caused by settlement, particularly in pumping zones (Herrera-García et al., 2021), or the mark of a natural or anthropogenic forcing of land emergence by controlled supply of sediment (Reed et al., 2009; Nienhuis et al., 2020). The southern coastal plain of the North Sea, which is the largest area of this type in Europe, does not escape this questioning (Koster et al., 2020). Groundwater management in the plain is a challenge (Ducrocq et al., 2022; Hauser, 2020), with the overexploitation of coastal aquifers leading inexorably to their progressive salinisation (Pauw et al., 2012; Lebbe et al., 2018), further accelerated by the retreat of the coastline (Ruz et al., 2009; de Winter & Ruessink, 2017).

This work, focussed on the French part of the Flemish coastal plain, addresses the relationships between the drainage and the geomorphological evolution of the Aa Valley, an estuarine system reclaimed in the Middle Ages and currently completely embanked down to the shoreline. The question posed is that of the stratigraphic recording of natural and anthropogenic forcings that occurred in the historical period, as they can be traced by archaeology and surface geophysics (Wilken et al., 2022). Since Antiquity, the Flemish coastal plain underwent profound surface transformations, with first heavy exploitation of peat in the Roman era, then reclamation in the Middle Ages, aiming at transforming the estuarine channel belt and associated tidal flats and salt marshes into a space entirely dedicated to agriculture (Verhulst & Gottschalk, 1980). Reclamation was achieved by embankment of the coastal plain distributaries, which paradoxically accelerated the drowning of polders that were thus starved of sediment and underwent peat compaction (Baeteman, 2018; de Haas et al., 2018). Besides this anthropogenic forcing, the contribution of natural forcings, like extreme events (storms and river floods), might be underlying, although not easy to unravel (de Kraker, 2015). These questions are

relevant in the modern perspective of increased storminess and rising sea levels (Ulbrich et al., 2019).

The objective of this article is to explore the stratigraphy of the last 4 m of sediment fill in a sector corresponding to the ancient estuarine border of the Denna, one of the distributaries of the French part of the Flemish coastal plain in the Middle Ages. This study, based on ground-penetrating radar and coring data, benefited from the results previously obtained during archaeological diagnostic campaigns carried out in the perspective of extension of the Grand Port Maritime of Dunkerque. It is the largest work in progress of this type in France, with a 10 km<sup>2</sup> area documented with conductivity maps, boreholes and pits, and archaeological materials collection and dating since 2015 (Lançon, 2017; Lançon, 2022; Desoutter, 2018, 2019, 2020; Deschodt et al., 2021). In this article, the morphology and stratigraphy of the uppermost deposits are explored over a subarea of 4 km<sup>2</sup>, and their evolution through the last millennium is interpreted as a possible response to land reclamation.

## 2 | BACKGROUND

The southern North Sea coastal plain, from Denmark to France (Figure 1A), is characterised by its low altitude, around 2.5 m above mean sea level, and sometimes even below sea level as in the Moères sector on the French–Belgium border (Figure 1B). In the French sector, it is backed by relief consisting of Meso-Cenozoic formations, 10–20 km behind the current coastline, and fringed seaward by an almost continuous coastal dune belt (Figure 1B). This coastal plain is made up of Holocene deposits that infilled and overflowed the palaeovalleys of the River Hem and the River Aa (Figure 1B), the general architecture of which was reconstructed from subsurface data (Margotta, 2014; Margotta et al., 2016). The water discharge of these rivers is very low, respectively 10 m<sup>3</sup>/s and 1.5 m<sup>3</sup>/s (IFREMER, 1986), and most of the sediments of the coastal plain were supplied from the North Sea via the Schelde and Rhine deltas (Figure 1A) (Hijma et al., 2009; Mathys, 2009). At present, these rivers are fully embanked and connected to a network of canals (Figure 1B), some of them being remnants of avulsed channels of medieval estuarine rivers (Figure 2A,B). The thickness of the Holocene deposits is *ca* 25 m near the

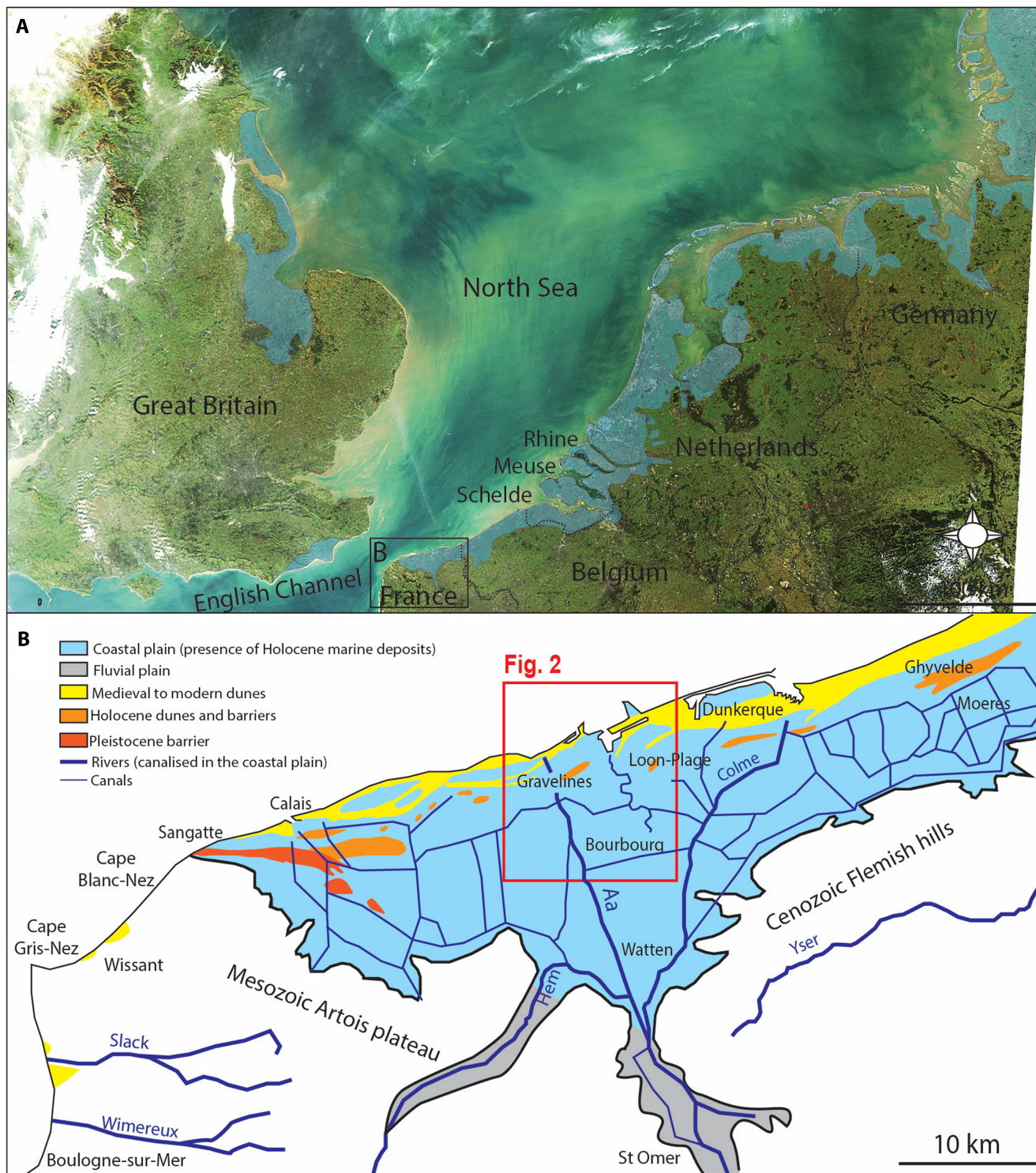


**FIGURE 1** (A) Holocene coastal plains of the Southern Bight of the Southern North Sea. The coastal area in blue corresponds to the contour of Holocene marine sediments in 1:200.10<sup>3</sup> to 1:10<sup>6</sup> geological maps of Great Britain, France, Belgium, Netherlands and Germany. (B) French coastal plain with main geomorphic features. Only the dunes at the present-day coast are locally still active. Modified from Sommé et al. (1999).

current coastline in the Gravelines region (Sommé, 2004). Beneath the Holocene, the coastal plain also includes continental Quaternary deposits related to the glacial Weichselian or the marine Eemian (Figure 2C).

Margotta et al. (2016) produced palaeogeographical maps showing a Holocene sequence consisting of a transgressive system tract dominated by sandy deposits of subtidal estuarine channels in the axis of the Hem/

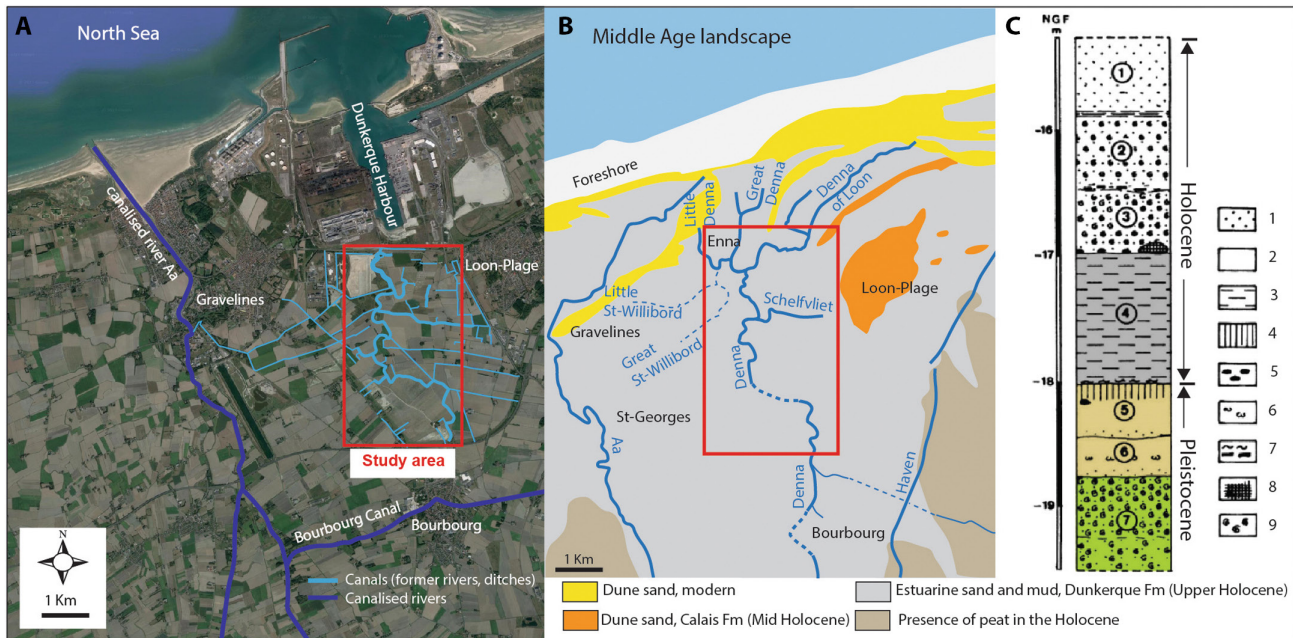


**FIGURE 2** Study area hydrographic network and coastal morphology at present (A) and as reconstructed in the Middle Age based on archaeological data (B, after M. Lançon and C. Cercy, INRAP). (C) Stratigraphic section of Quaternary deposits observed during excavation of Dunkerque harbour, 1 km north of the study area. Modified from Sommé et al. (2004). Lithological units in circles. Caption of facies in the original publication: 1: lithological units, 2 and 3: sand, 4: loam, 5: clayey loam, 6: organic soil, 7: pebbles, 8: calcareous concretions, 9: vegetal remains, 10: peat, 11: shells (marine molluscs).

Aa palaeovalley and a highstand system tract dominated by deposits of muddy foreshore, both punctuated by peat layers at the coastal onlap. The study area, in the axis of the main Holocene estuarine rivers, is devoid of peat (Figure 2B). These two system tracts are separated by a tidal ravinement surface formed around 5500 cal yr BP just before the sub-boreal period (5000–2800 cal yr BP), representing the maximum extension of peat on the Belgian side (Baeteman & Declerck, 2002). The top of that peat could correspond to the maximum flooding surface of the Holocene, established at 2800 cal yr BP close to present-day sea level (Lambeck et al., 2002). Near the current coastline, in the study area, the transgressive Holocene corresponds to a metre-thick layer of marine silty clay overlain by 17 m of sands with a large number of marine shells at the base (Figure 2C).

The highstand system tract records the fluctuations of the estuarine environment, in particular the Dunkerque ‘transgressions’ marked by *Cardium* levels (Dubois, 1924) and associated with climate fluctuations by Ters (1973). More probably, the Dunkerque I (2800 cal yr BP), Dunkerque II (3rd–6th century) and Dunkerque III (9th–12th century) shell-rich layers were supplied during the cold episodes of increased storminess in the North Sea, separated by warm and calm periods of the Roman and Medieval Climatic Optimum, reflecting Holocene climate changes in Europe (Wanner et al., 2008). On the other hand, human activities in the

coastal plain (peat exploitation, land reclamation) could also explain some of these fluctuations. In particular, it is possible that peat extraction by the Romans induced an increase in accommodation, thus being able to give the illusion of a transgression in Dunkerque II strata (Baeteman, 2007).

In Antiquity, only mounds (‘terpen’) were occupied because the plain was still regularly flooded by the sea (Nieuwhof et al., 2019). As was already assumed in the 17th century, the estuarine rivers in this area probably formed a distributary system, the Aa delta, the main rivers of which can be traced around the study area (Figure 3). The book featuring this map was used in the 17th century for management and political strategy, and is not indicative of the arguments supporting the palaeo-river geography, but the main features of the map are consistent with the present-day lowlands and old river courses. In the Middle Ages, land reclamation was accelerated by the development of dikes and canals (Hoeksema, 2007).

The Aa delta formed an anastomosed network of estuarine rivers that have been progressively embanked and connected by straight canals parallel to the coast (Figures 1B and 2A), named ‘wateringues’ in the local language (from ‘Watergangs’, waterways). The canals, originated as ditches, were dug at the border of dikes which were probably the product of these excavations but also served as communication paths in the wetlands (Lançon & Boulen, 2019).

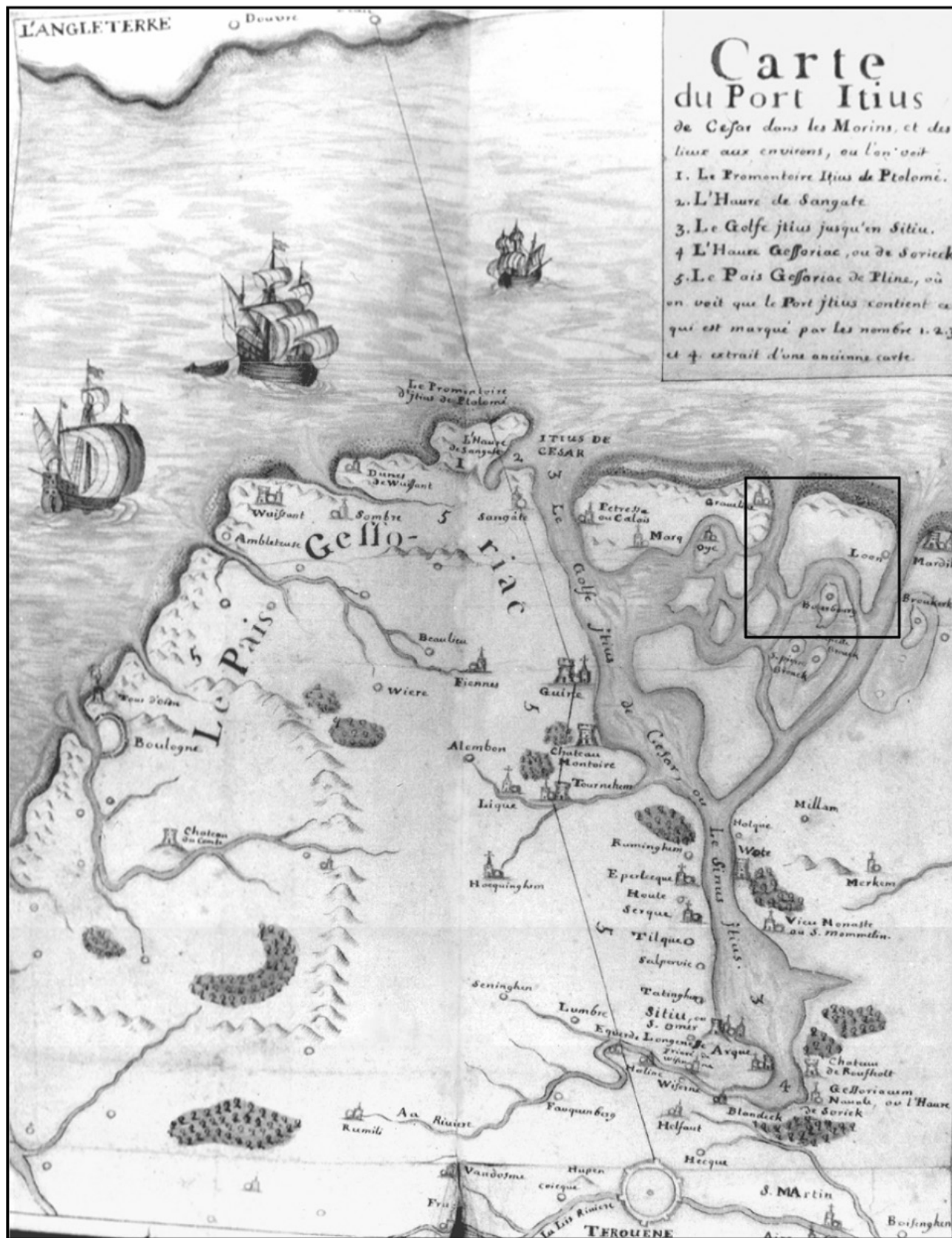


FIGURE 3 Map from 17th century picturing the Aa delta and other features of the Flemish coastal plain like people of that time could imagine it was in Antiquity. First published in Latin by Jacques Malbrancq 'De Morinis et morinorum rebus', 1639, Tournai, and then copied numerous times in French. This one is exhibited in the city museum of St Omer. The inset black frame approximately corresponds to the area in Figure 2A,B.

The Dunkerque ‘transgressive’ strata are all older than land reclamation, despite the presence of a renewed episode of cold and stormy climate during the Little Ice Age (15th–17th centuries), similar to that in Dunkerque I and II (Clarke & Rendell, 2009). This reinforces the hypothesis that land reclamation was taking over natural processes in the geomorphological evolution of the coastal plain. The main objective of this article was to provide data for assessing the key controls of the final emersion of the estuarine landscape, based upon its geological record. Therefore, a study of the architecture and sedimentology of the last 4 m of the coastal plain was undertaken, in an area bordering the last distributary of the Aa delta, the medieval Denna River (Figure 2B).

### 3 | DATA AND METHODS

The data used in this study are reported in Figure 4.

#### 3.1 | Electrical conductivity

This method allows mapping of contrasted near-surface lithologies, deciphering in particular the amount of clay (more clayey soils being more conductive). The survey was carried out by the National Institute for Archaeological Research (INRAP), with a CMD Explorer system (from GF Instrument), equipped with a transmitting coil set at 10 KHz and three receiving coils located at distances of 1 m, 2 m and 4 m from the transmitting coil. The apparent electrical conductivity was mapped at investigation depths of 1.5 m, 3 m and 6 m. To ensure high positioning accuracy, a differential GPS (Trimble with Téria network correction) was used. To avoid electromagnetic interference, the acquisition system was placed on a sled towed by a 4×4 vehicle located a few metres from the device, with the CMD Explorer placed at a height of 25 cm above surface.

#### 3.2 | Ground-penetrating radar

Ground-penetrating radar (GPR) is a technique widely used to obtain images of the near-surface geology. The GPR profiles were obtained after agricultural soil was stripped from 50 cm deep archaeological trenches, allowing better coupling of the antennas on the sediment (Figure 5A). A GSSI acquisition system was used, including a SIR4000 control unit and 200 MHz and 350 MHz antennas (Figure 5B). In total, 42 km of GPR profiles were acquired with a spacing of 20 m during two campaigns (Figure 4A). A penetration of up to



**FIGURE 4** (A) Map of GPR profiles collected (black lines). The pit is that illustrated in Figure 15. Basemap: the near-surface conductivity is mapped above satellite image. (B) Detail of the square frame in A. In red (P1–P4), GPR profiles illustrated in Figures 9 and 10. C1–C5: vibrocores logged in Figure 12.

4 m was obtained on 15% of the profiles produced. In addition, INRAP acquired high-resolution topographical data using a DGPS, which were used to reconstruct the two-dimensional GPR profiles. To process the data, the Radan and GPRpy softwares were used for making zero-time adjustments, removing background noise, converting times to depths, performing migration and correcting topography. For the time-depth correction, a speed of 0.087 m/ns was set up, corresponding to a dielectric constant of  $12 \text{ F.m}^{-1}$ , based on the analysis of reflection hyperbolas (Bristow & Jol, 2003). This value is adapted to a wet sand deposit, given that the GPR acquisition was carried out in autumn, in rainy conditions (Figure 5B).

**FIGURE 5** (A) Archaeological diagnostic trench showing inclined heterolithic stratification. The GPR profiles were acquired along the trenches to avoid the masking effect of the clay and organics-rich soil. (B) The GSSI GPR 350HS and SIR4000 equipment. Profiles collected during rainy days are of lesser quality. (C) This light vibrocorer allows remote places of the coastal plain to be accessed for the collection of up to 6 m-long cores.



### 3.3 | Vibrocores

The cores were collected with a vibrocorer built in the laboratory. It is a lightweight device, with an aluminium tube 8 cm in diameter, held on a ladder by guy wires and vibrated by a jackhammer head powered by a generator (Figure 5C). Five cores were collected along the GPR profiles previously carried out, choosing the locations according to the anomalies observed on the GPR profiles and the apparent conductivity maps (Figure 4B). The cores were collected after the archaeological trenches were filled, which explains why the upper part of each core is made up of freshly reworked soil with a sharp erosional bottom. In addition to the visual description of the cores opened in the laboratory, sampling was carried out (every 20 cm for core 02 and every 10 cm for core 05) for grain-size analysis (Malvern Mastersizer), for description using a binocular magnifying glass (1 cm<sup>3</sup> per sample) and for meiofauna study (8 cm<sup>3</sup>). The samples prepared for meiofauna were sieved into fractions ranging from 315 to 63 μm. Additionally, methylene blue cleaning was performed to improve identification

and facilitate counting of foraminifera present in the samples.

### 3.4 | Outcrop

By the end of this project, an archaeological pit was dug across a structure revealed by the archaeological prospecting (location in Figure 4A). This pit crosscuts the sedimentary units imaged on the GPR profiles and provided field-based additional observations that are reported herein.

## 4 | RESULTS

### 4.1 | A surface network of mud-fill channels, ditches and depressions

The electrical conductivity map highlights natural lithological contrasts or anthropogenic infrastructures (Figure 4A). Electrical conductivity values range from 10 to 40 mS/m. This range of values indicates a relatively resistant soil,



mainly consisting of sand (Doolittle & Brevik, 2014). Strong contrasts are observed at the boundaries of plots where agricultural use differs (wastelands, crops, roads, etc.), but this does not prevent the observation of underlying discontinuities of geological or anthropogenic origin. The anomaly maps produced at different depths (1 m, 3 m and 6 m) do not show any significant difference (Figure 6), which suggests that the conductivity contrasts are mainly carried by deposits close to the surface (between 0 m and 2 m). Buried irrigation networks, for example, can be identified and have been confirmed by archaeological prospecting (Desoutter, 2018). The areas of higher conductivity can express the increase in salinity or clayeyness of the land. Salinity was not measured but the structures that the mapping reveals show that these higher conductivity areas are channel fills or heterolithic deposits interstratified in channel bars. The most superficial ones are also observed on aerial images in many places on the Flemish coastal plain, particularly in spring when the difference in cereal growth directly reflects the water content of the soil and therefore the amount of clay (Figure 7).

The highest amount of clay, continuous over large areas, is observed at the north-western limit of the explored area,

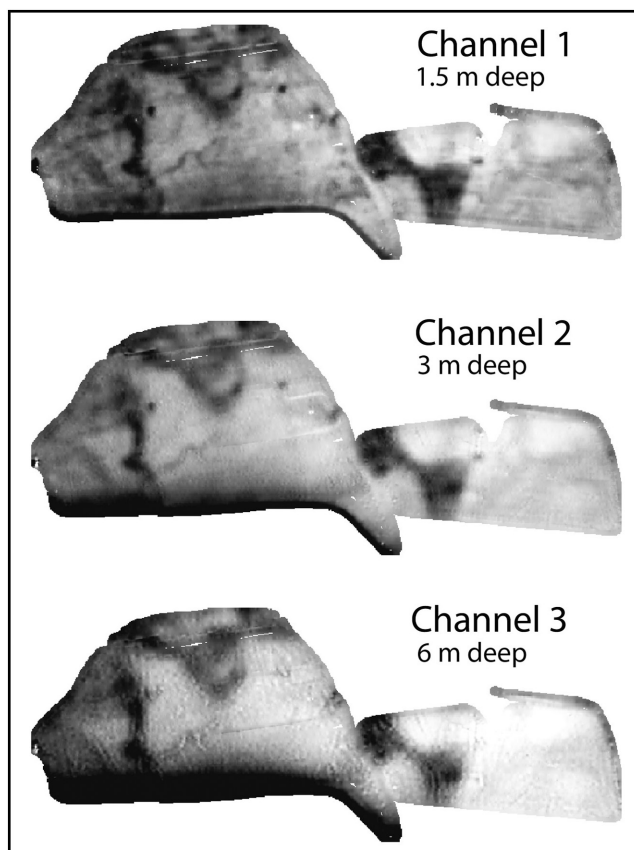


**FIGURE 6** Conductivity maps extracted at various depths, showing a decrease in resolution with depth but without change in pattern. This means that conductivity contrasts reflect near-surface deposits. See location in Figure 4A.

and probably extends well beyond to the west, towards the canalised River Aa. The main high conductivity areas correspond to a major channel system, several hundred metres wide (Figure 8). The central and eastern part of this system is sandier on average, crossed by small tributaries around twenty 20 m wide on average and highly sinuous (sinuosity of 1.3 on average). The flat sandy areas between the channels are traversed by minor creeks 1 m wide, as a result of final drainage. In addition to the surface channel system, north-south alignments of high-conductivity circular anomalies are observed. The information provided by archaeological campaigns show that these features are mud-filled ponds, which are aligned along the medieval dikes. The relationship between the dikes and those ponds is discussed below.

## 4.2 | From point bars to vertically accreting deposits

The GPR profiles provide a stratigraphic view of the surface formations identified on the apparent electrical conductivity maps, and reveal buried units (Figures 9 and 10). Penetration reaches 4 m, except in the clayey fill of channels or in areas where soil salinity is higher. In those areas, penetration can fall to zero. Three stratigraphic units are observed, uniformly distributed throughout the area.

### 4.2.1 | Unit 1

This is the deepest unit. Its base is not defined (beyond the penetration limit). It is constituted by the amalgamation of overall aggrading sediment bodies bounded laterally and vertically by erosion surfaces. In cross-sections, these sediment bodies, up to 2 m thick and several tens of metres in lateral extent, are made up of inclined strata that build flat-based bodies (Figure 9; P2, 240–280 m) or infill scours (Figure 9; P2, 170 m). In comparison with the sinuous planform geometry of the channels in the conductivity map, these sedimentary bodies can be interpreted as channel fills and point bars formed by lateral accretion. The sinuous character of the related channel system is supported by the cut-and-fill pattern of bars with opposed accretion directions (to the east or west in those east-west profiles). The apparent slope dip of accretion surfaces is 10°, which underestimates their real slope but is consistent with the slopes observed in small estuarine point bars (Choi et al., 2013).

### 4.2.2 | Unit 2

This unit, present between 1.5 m and the surface, rests on Unit 1. This is the depth range with the maximum

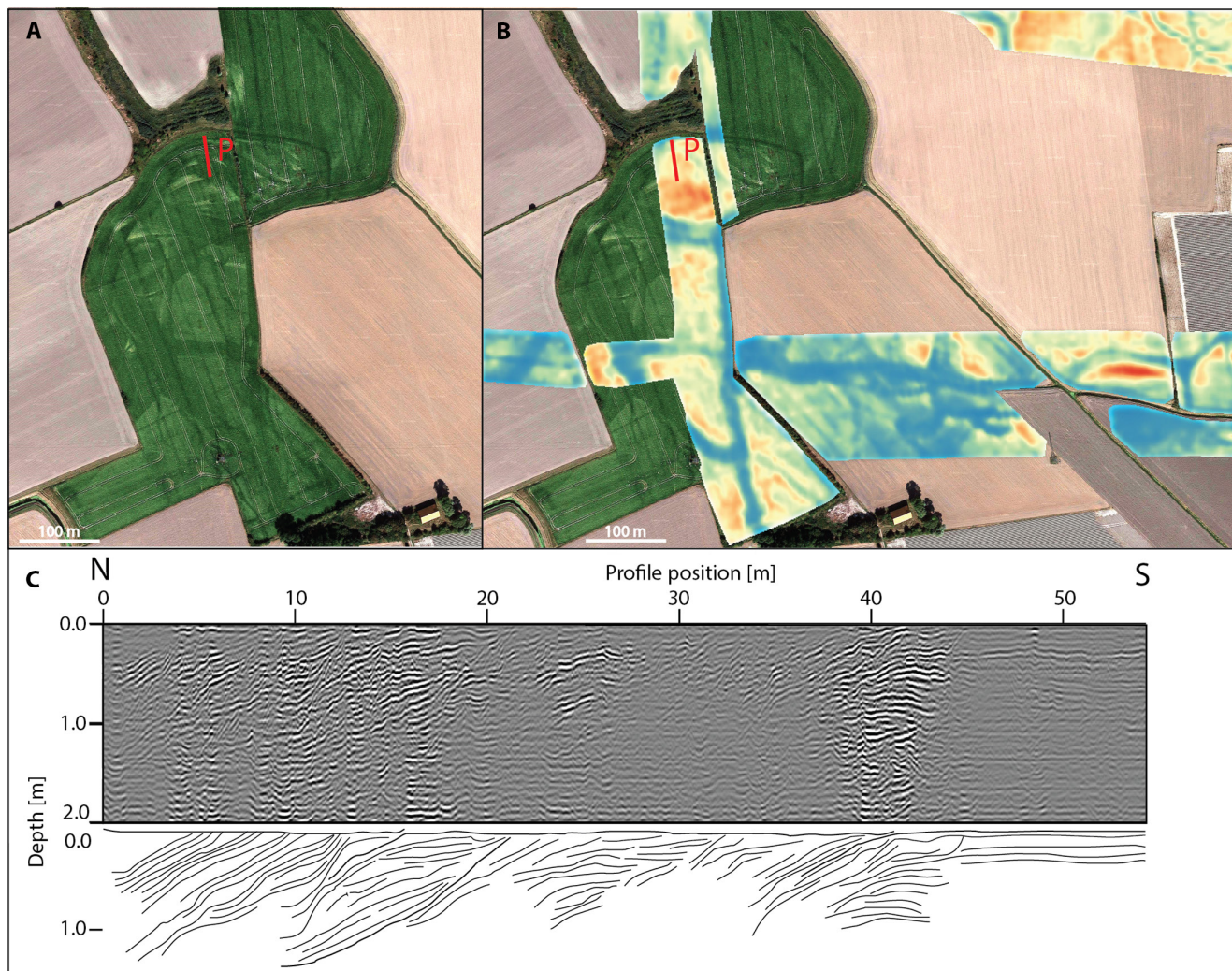


**FIGURE 7** (A) Satellite image of a grass field in spring (surrounded by ploughed fields). See location in Figure 4A. Contrast has been increased so that the surface network of buried channels appears, enhanced by variation in clay content in the soil. (B) Same area with superimposed conductivity map. The clayey channel plugs can be mapped in detail throughout the entire study area. (C) GPR profile showing the inclined heterolithic stratification of a point bar (P section in A and B).

conductivity contrast (Figure 6). Unit 2 is distinguished by almost continuous horizontal reflectors, corresponding to aggrading deposits, the interpretation of which is discussed below. They are locally intersected by metre-deep and up to 40 m wide channels. These channels are generally filled in one phase but can locally be multi-storey (Figure 10; P3 at 30 m). The aggrading deposits of Unit 2 between the channel fills have overall low conductivity, which suggests they are sandy. The channel fills are more conductive (Figure 9; P2 at 280–300 m, compare with Figure 4B). They show concave-up or lateral accretion infills, with interstratified mud layers as evidenced in archaeological trenches (Figure 5A). These heterolithic stratifications are the characteristic of tidal channels in most estuaries of the southern North Sea (Donselaar & Geel, 2007). Unit 2 thins towards the main tributary channel of this part of the estuary, located to the west of the

area, and also locally towards the margins of the smaller channels embedded in the unit (Figure 9; P2). This thinning is correlated with the rise of the bottom of the unit, the top of which is horizontal.

#### 4.2.3 | Unit 3

This is a thick unit but occurring only locally and difficult to image due to strong attenuation of the signal, which suggests a significant proportion of clay in the sediments. On some profiles, however, it shows faint inclined stratification, with a slope locally exceeding 10°, and incision over >1 or 2 m in the lower units (Figure 10; P4, 0–40 m). This architecture is interpreted as inclined heterolithic stratification, a characteristic of lateral accretion in large-scale point bars (Thomas et al., 1987). Although the

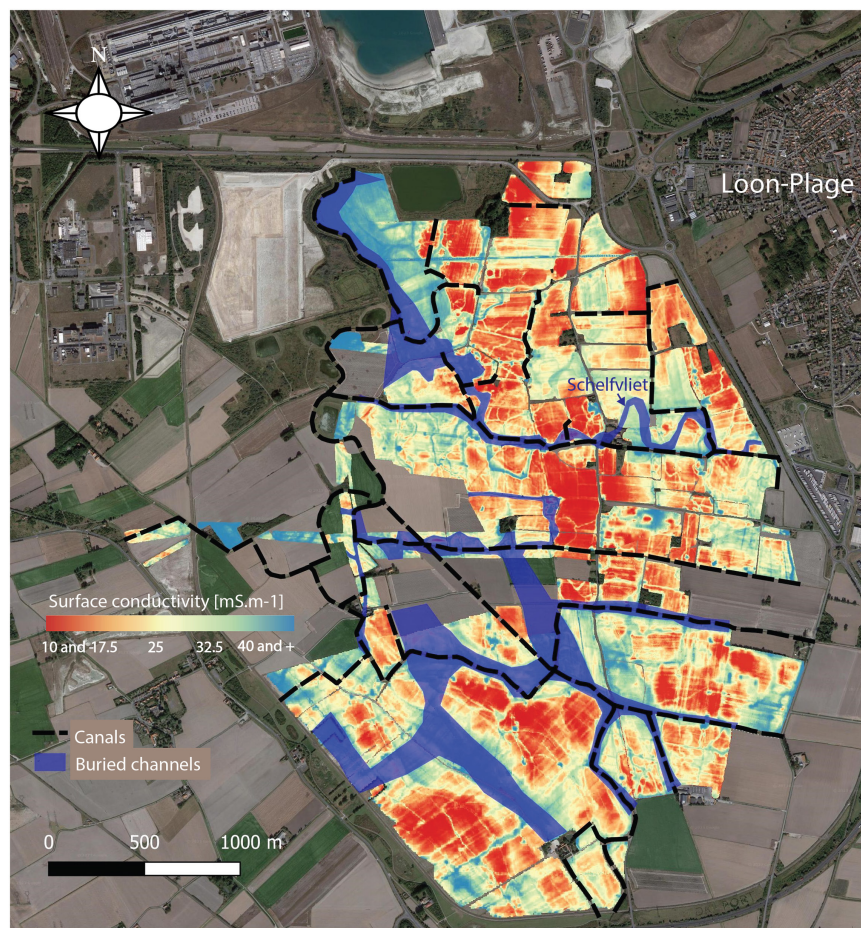


**FIGURE 8** Conductivity map, with buried channel network highlighted in blue. The meandering channel heading westward, and then northward in the NE part of the surveyed area is the Schelfvliet (see Figure 2B). The channels have been progressively embanked during the Middle Age. Some bends or discontinuities in the channel pathways may result from reclamation.

bottom of the channel is not imaged, this interpretation is in accordance with the location of the profile across the convex edge of a meander of the main tributary channel, the width of which is 200 m in that area according to the conductivity map (Figure 8).

The mapping of some of the channel fills based on GPR profiles (around 30 km out of the 41 km of profiles produced), although fragmented due to (i) the limited extent of coverage, and locally (ii) the poor quality of the data or the (iii) truncation by later channels, reveals part of the morphology and distribution of the channels not visible on conductivity maps (Figure 11). The complexity of Unit 1, entirely made up of cut-and-fill channel bars, means that only a few major channels could be followed and mapped. The channels in Unit 1 are wider than those in Unit 2, possibly a consequence of their higher lateral mobility as the width of the mapped channels encompasses their lateral migration. All the channels have a main north–south orientation, along the route of the Denna River (Figure 2). Both lateral accretion and centripetal infilling is observed (Figure 11). Centripetal infilling is where both facing channel banks are buried beneath inclined strata, finally merging into a concave-up succession of strata plugging the channel. While lateral accretion dominates in Unit 1 (for it

is composed of point bars), centripetal infilling dominates in Unit 2. This evolution is classically observed along with a clayeyness increase upwards in tidal flats (Makaskee & Weerts, 2005; Hugues, 2012).

### 4.3 | Progradational tidal flats with marine and possibly aeolian supply

The vibrocores contain three main facies (Figure 12). The first facies, preserved below the reworked horizon of agricultural soil, is either a beige sand with iron oxide precipitation fronts, or, a darker silty-clayey sediment with gleys (nodules formed by iron oxidation of the lesser permeable matrix). The sand bears veneers of bioclasts of *Cerastoderma edule*, numerous *Hydrobia*, and unidentified plant elements, some transported and others in place (roots). Some concentrations of mud clasts are also observed. The base of the cores consists of a grey sand facies, the top of which is located about 1.5 m below the surface. This facies is interstratified with either centimetre-thick layers with a higher mud content, or slightly coarser grained decimetre-thick layers with more abundant shell clasts (bivalves and gastropods). Entire *Cerastoderma edule* shells in life position, or with valves connected are

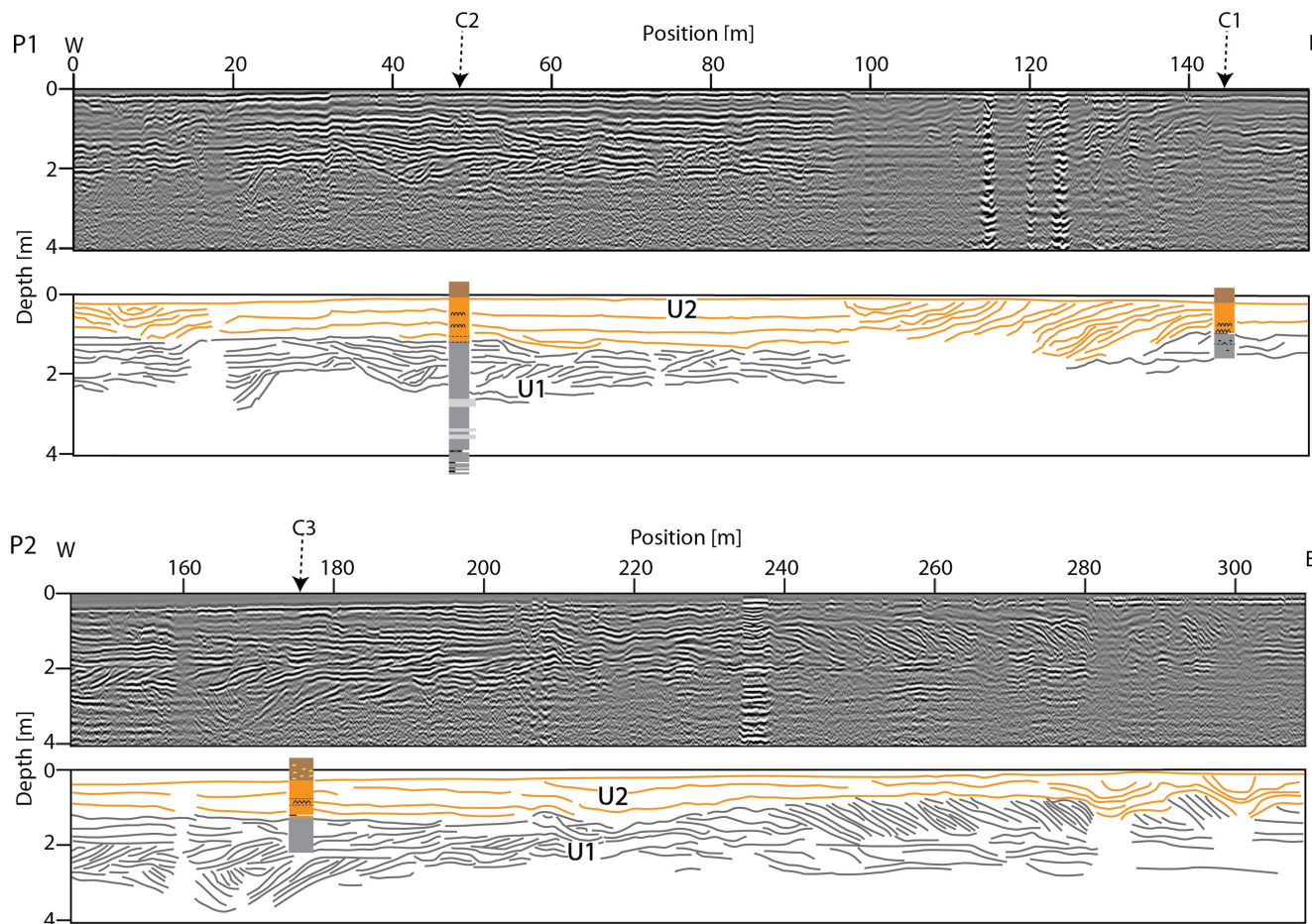


**FIGURE 9** GPR profiles P1 and P2 (see location in Figure 4B). Two main units can be followed throughout the surveyed area: U1, fully channelised, and U2, with sparse channels incised in flat strata. C1, C2 and C3: vibrocores (see Figure 12).

also present in this facies. The facies are generally devoid of sedimentary structures in cores.

The grain-size analysis of 24 samples dominated by sand (core 4) and eight samples dominated by silty clay (core 5) shows a good consistency of grain-size distribution from one sample to the other upward in the cores, and an overall evolution with no change across the grey to beige sand boundary (Figure 13). The sands have a mode around 110µm, with good sorting. Upward in the cores, sorting gradually decreases together with an increase in positive skewness, indicating a progressive increase in the amount of cohesive silt fraction (10µm). This fine-grained silt fraction is probably that forming the mud clasts and drapes in the cores.

Under the binocular loupe, the grains are mainly composed of quartz (Figure 14), with a majority of shiny grains, which is typical for sands evolved in a marine environment. However, a small fraction (1%) of well-rounded, sometimes frosted grains indicates a possible aeolian contribution (Krinsley & Trusty, 1985). Bioclastic grains, less than 3% of the total sands, allow the identification of sponge spicules and echinoderm fragments (Figure 14B,C), indicative of a marine source for the sand. In the mud layers, foraminifera

of the genus *Ammonia* are present (Figure 14D), indicating an estuarine (brackish) environment. The *Hydrobia* present in the beige sand are also indicative of intertidal estuarine environments as they are subject to desalination. The interpretation of an estuarine deposit is consistent with the presence of *Cerastoderma edule* in life position, as these organisms are also tolerant of salinity variations (Malham et al., 2012; Peteiro et al., 2018). The sediments of the silty-clayey facies in core 5 show a greater diversity of biota. In addition to the molluscan faunas already present in the sands, ostracods (Figure 14F) and diatoms (Figure 14E) are found. Foraminifera include *Haynesina germanica*, *Criboelphidium* (*williamsoni* and *gerthi*), *Quinqueloculina* seminula and the *Ammonia* group (Figure 14F), confirming the estuarine signature of the depositional environment (Armynot du Châtelet et al., 2019).

#### 4.4 | Tidalites infilling scoured depressions

A 5 m deep and 30 m long pit was excavated in October 2023 across one of the high-conductivity circular

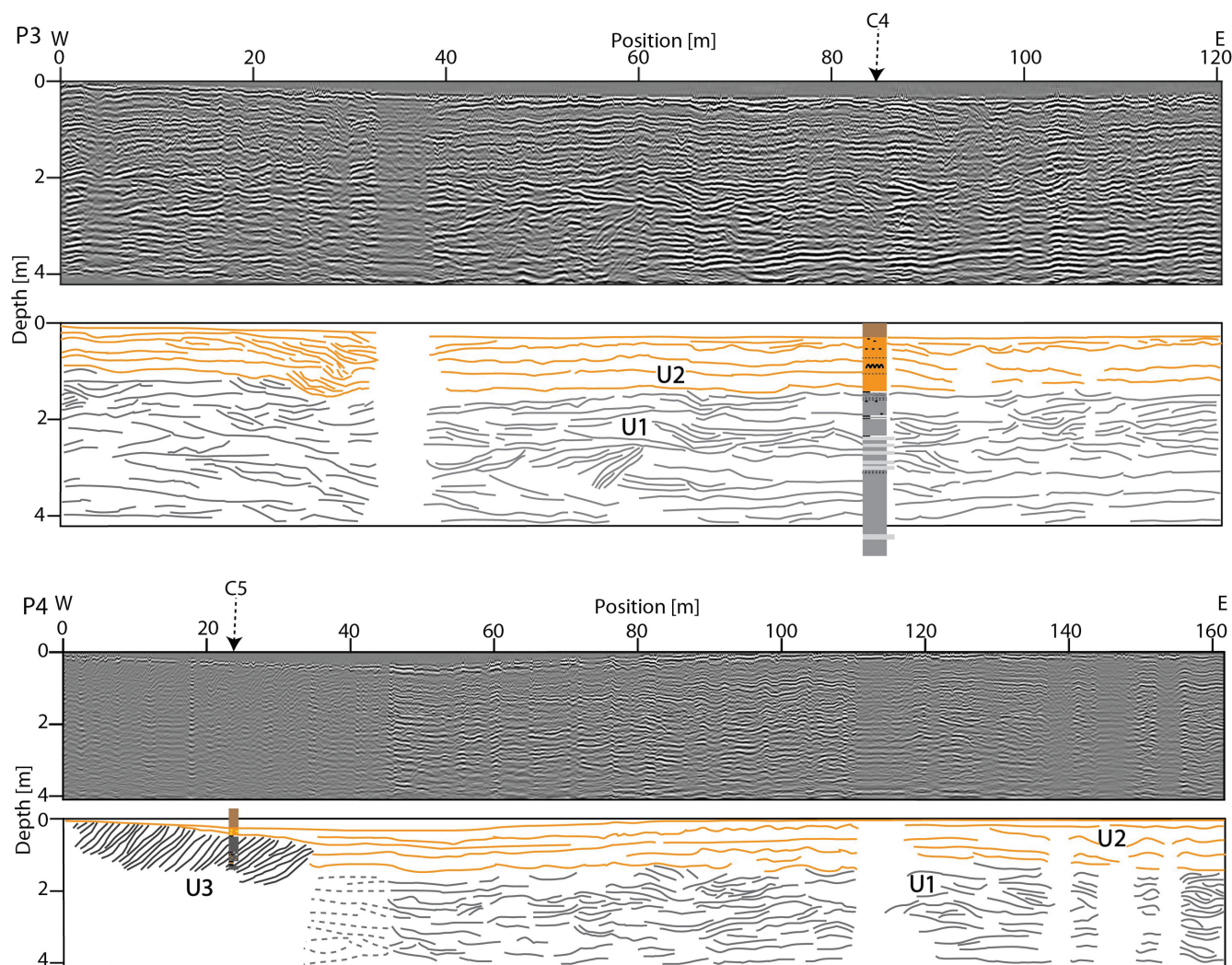


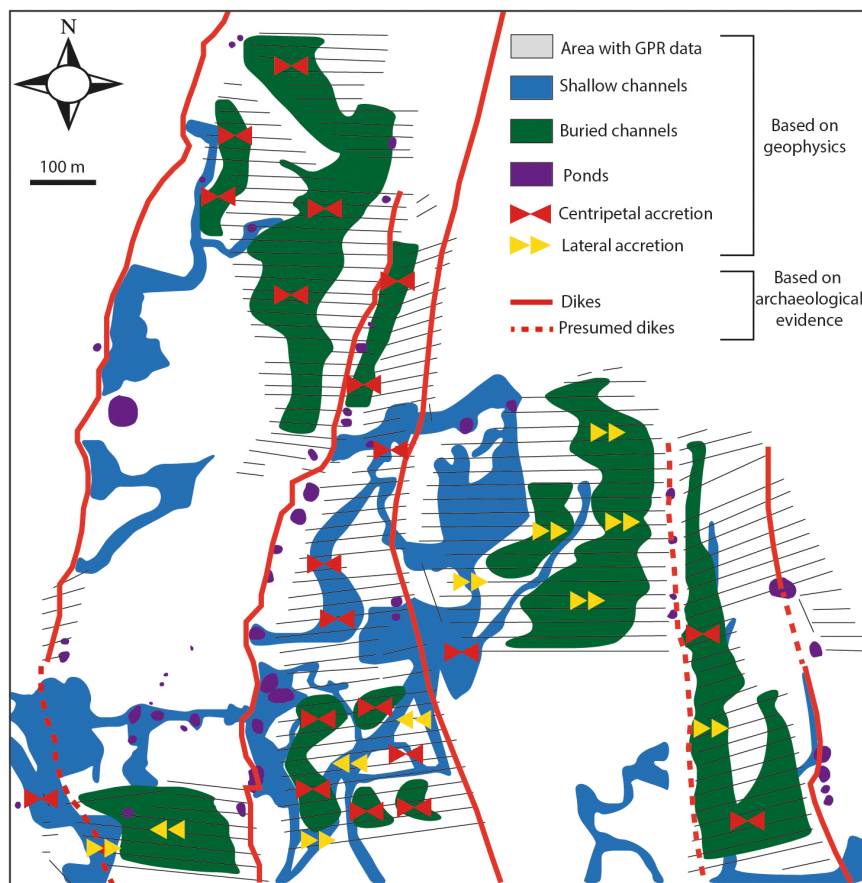
**FIGURE 10** GPR profiles P3 and P4 (see location in Figure 4B). Penetration in sandy areas can reach 4 m across U2 and U1. In clay-rich areas, such as those with thick silty-clayey channel fills (U3 in P4), penetration is much reduced and the signal is noisy. C1, C2 and C3: vibrocores (see Figure 12).

anomalies, confirming they are mud-filled depressions (Figure 15). In this pit, the deposits below the incision consist of a grey-to-beige succession interpreted as the same as that identified in the cores. The 30 m wide exposure of the pit allows the structure of these facies to be documented, something that is almost invisible in the cores. The mud-filled depression is floored by an erosional scour, 5 m deep (Figure 15A,B).

The grey sand is composed of, from bottom to top: (i) trough crossbeds a few decimetres-thick floored by *Cerastoderma edule* lags, cross-cutting low angle masterbeds of dominantly tabular bedding (Figure 15C); (ii) decimetre-thick sets of low-angle planar to arcuate crossbeds bounded by flat ripples; (iii) very-low angle 5 cm thick sets of ripple cross-stratification, traversed by post-depositional rootlets. Beds of type (ii) and (iii) interstratify, and opposite migration directions are noted in the ripples and crossbeds (Figure 15D). Palaeocurrents deduced from

the ripples and trough crossbeds are dominantly towards the south-east. At the top of the grey sand, the very low angle master bedding in the ripple sets disappear, the ripples being amalgamated over 30 cm, and highlighted by flasers (Figure 15E). The grey sand then grades upward first to a beige heterolithic package of wavy to flat strata (alternations between 2 cm and 10 cm thick layers of sand and clay), progressively perturbed upward by bioturbation (roots), desiccation cracks and possibly trampling (Figure 15F). A redox front of iron lixiviation is found in this level, 80 cm below the surface, explaining the grey to beige change in colour. This succession is finally covered by a structureless, whitish sand forming the last layer of the section exposed in the pit, about 50–70 cm below the surface (which is the thickness of soil that was stripped off before the onset of archaeological work). The top surface is locally incised by ditches infilled by massive, organic-rich mud with *Scrobicularia* (Figure 15H).

**FIGURE 11** Reconstructed network of channels and canals. Some large buried channels are abruptly terminated, possibly due to embankment during land reclamation. Some terminations, however, are due to a lack of data. Old dikes were built along buried channels. Some recent channels crosscut the dikes, suggesting those ones are more recent. Due to the absence of NS profiles, the true geometry of inclined accretion surfaces could not be determined and the arrows only indicate apparent migration.



Based on these observations, the crossbedded grey sands could correspond to Unit 1 in GPR profiles, and the overlying flat strata in the beige to whitish deposits to Unit 2. In contrast to that observed in the GPR data, but consistent with observations in cores, the transition from the grey to beige sand might be gradual at this place. The crossbed sets at the bottom of the grey sand are formed by dunes migrating in the channels. The south-east-directed palaeocurrent suggests the possible influence of flood currents in the channels of Unit 1, something expected in the outward part of tide-dominated estuaries (Dalrymple, 1992). The upward grading to ripple cross-stratification is consistent with the overall decrease in energy upward a point bar, and the masterbedding formed by the ripple cross-sets correspond to the epsilon master bedding of the point bars (Smith et al., 1988), a detail that could not be seen in the GPR profiles. The flasers preserved in the upper part of the rippled sediments record the transition from a sand to mixed tidal flat, and correspond to slack water stages of the high tide (Reineck & Wunderlich, 1968). The overlying heterolithic strata would correspond to the wavy bedding of a mixed flat, progressively muddier upward.

The muddy deposits infilling the scour depression are composed of couplets of fine sand (minor part) and silty clay (major part) laminae, draping the slope of the scour

and progressively compensating the trough. They form upward-thinning bundles, about 10 cm thick on average, each comprising 12–14 couplets (Figure 15G). The laminae are thicker in the middle part of the bundles, where double-mud couplets are locally preserved (a very thin veneer of clay coring the sand laminae). They thin towards the bundle boundaries, where the sand laminae almost vanish and couplets amalgamate into a muddy layer. These heterolithic deposits are interpreted as tidalites, implying that the scour depression was connected to the latest tidal channels, probably those interpreted as infilled by muddy heterolithic strata (Unit 3). The bundles are interpreted as neap-spring cycles similar to those in the vertically accreted sand-mud laminae that are common in the upper part of the infilling of muddy tidal creeks (Roep, 1991), or on tidal flats where planar bedding dominate (Tessier, 1993), or even in large ponds of coastal swamps (Kvale et al., 1989). The occurrence of double-mud couplets suggests that two slack-water stages may be recorded during spring tides, suggesting that the bottom of the pond remained flooded. The much thinner mud laminae in the core of the double-mud couplets could be the result of diurnal inequality, which might be amplified in the internal part of estuaries (Gong et al., 2016). Considering a semi-diurnal tide, only half of the cycles are recorded as couplets. This could be the result of non-flooding of the pond during neap tides,

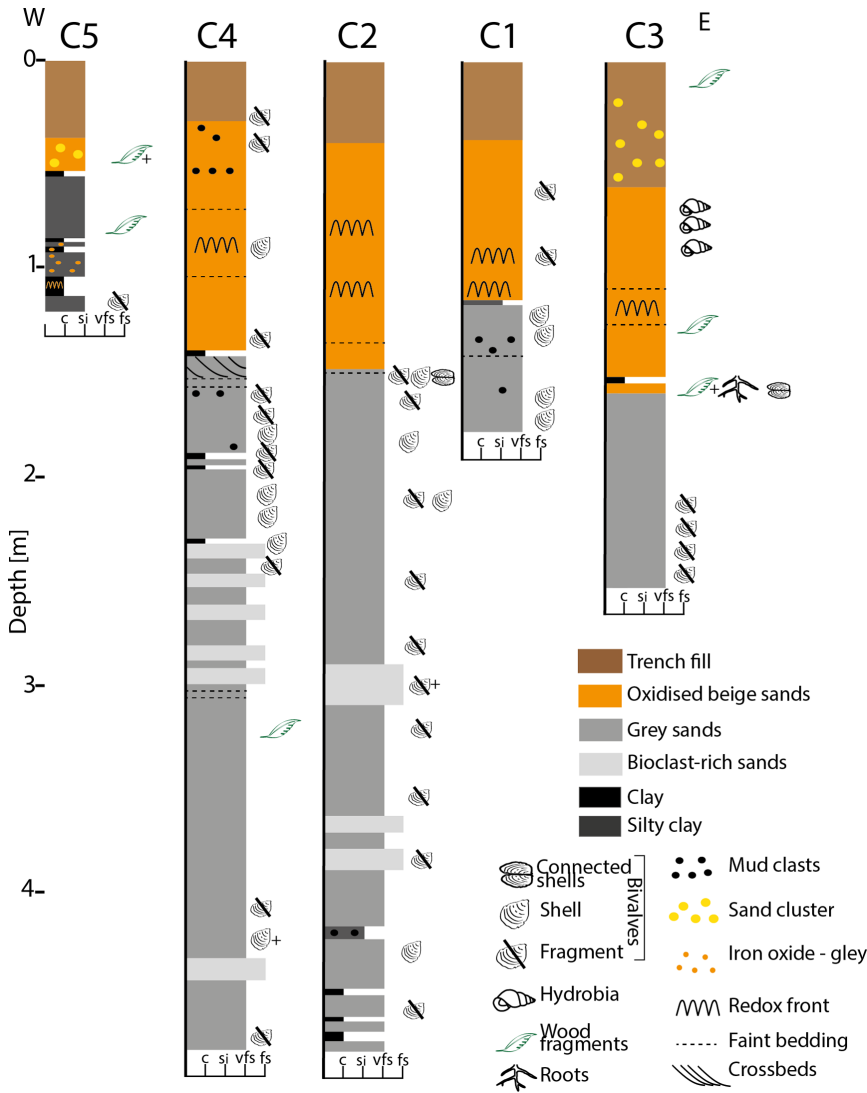


FIGURE 12 Vibrocore logs. See location in Figure 4. Two main facies are observed, based on iron redox change. The boundary approximately matches that of U1 and U2 in GPR profiles.

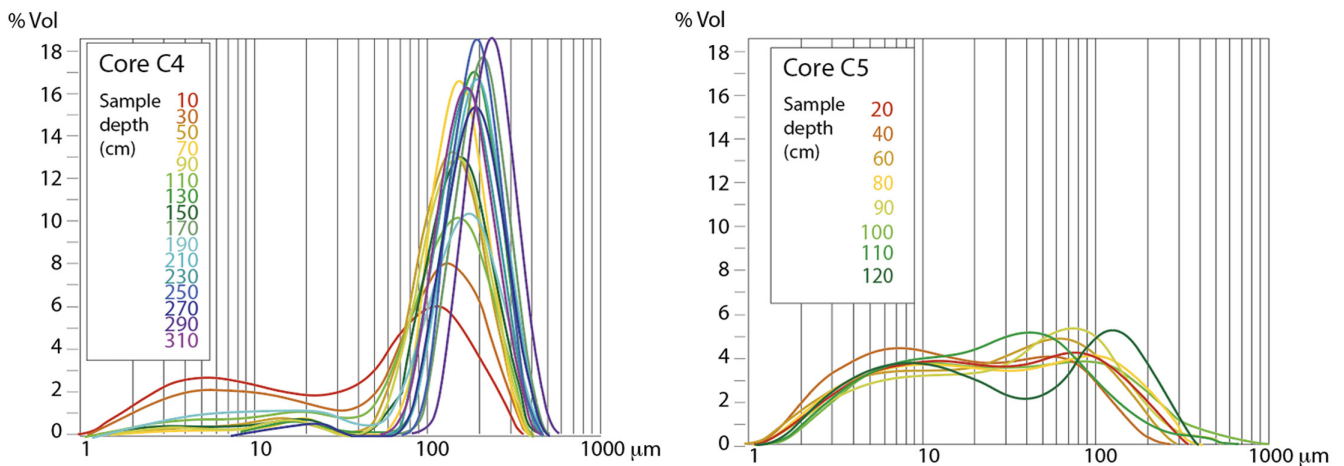
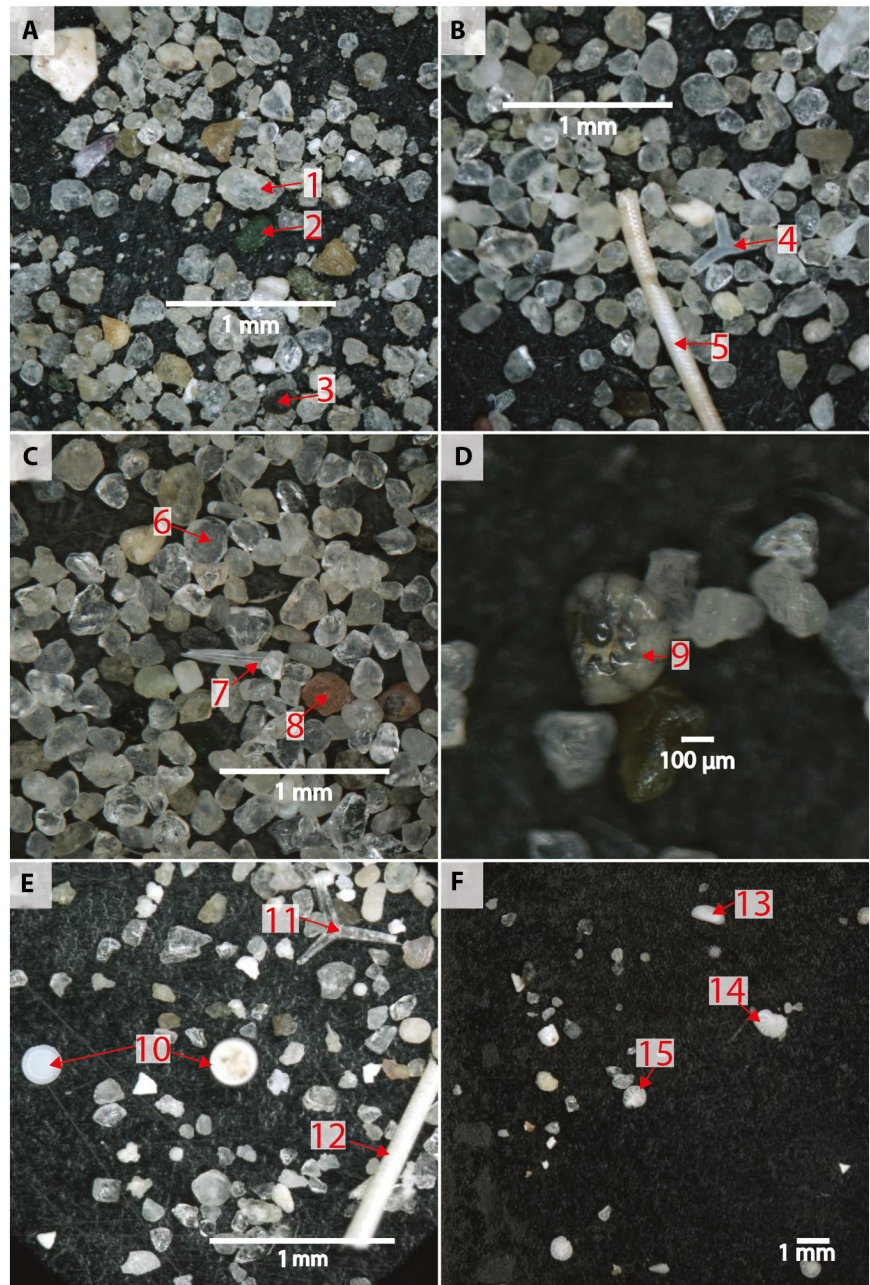


FIGURE 13 Grain-size variation with depth in cores C4 and C5. There is an overall fining-upward of the sand mode (120->100 μm), typical of tidal flat sediments (C4). The silts (3–10–20 μm) dominate over the sand in the muddy channel fills (C5). Grain-size distribution at the surface is homogenised by ploughing.

**FIGURE 14** Photographs of samples taken from cores C3 and C5 (see Figure 13). (A) C3 at 0.45 m (1: shiny quartz, 2: glauconite, 3: lithic fragment). (B) C3 at 1.65 m (4: sponge spicule, 5: echinid spine). (C) C3 at 2.05 m (6: frosted quartz, 7: echinid spine, 8: lithic fragment). (D) C3 at 2.05 m (9: *Ammonia*). (E) C5 at 0.70 m (10: diatoms, 11: triactin sponge spicule, 12: echinid spine). (F) C 5 at 0.95 m (13: ostracod, 14: *Haynesina germanica*, 15: *Criboelphidium williamsoni*).



or to amalgamation of the cycles in the bundle boundaries where sand laminae are almost absent.

## 5 | DISCUSSION

### 5.1 | Natural estuarine sedimentation and land emergence

Unit 1 in GPR profiles and in the pit exposure corresponds to the facies of grey sands dominated by channel processes. This may explain the presence of several scales of crossbedding (Figure 15B,E). The absence of systematic crossbedding in the sands collected in cores may be due to

disturbance of structures during vibrocoreing. The clarity of the GPR signal in this unit is consistent with the sandy composition. The occasional clay drapes observed in cores are probably too thin to impede the signal propagation. The beige sand in the pit section suggests that it is the upward transition from heterolithic tidal flat to salt marsh, where bioturbation processes progressively overprint the tidal bedding, with trampling of deformation features that could be created by cattle, as evidenced in the tidal marshes of the Frisian islands (Bakker et al., 2023). The succession of units shows a change in dynamics, transitioning from a high-energy system entirely occupied by sandy channels and meander bars (Unit 1) to a low-energy system with fewer channels, flat deposits (Unit 2;



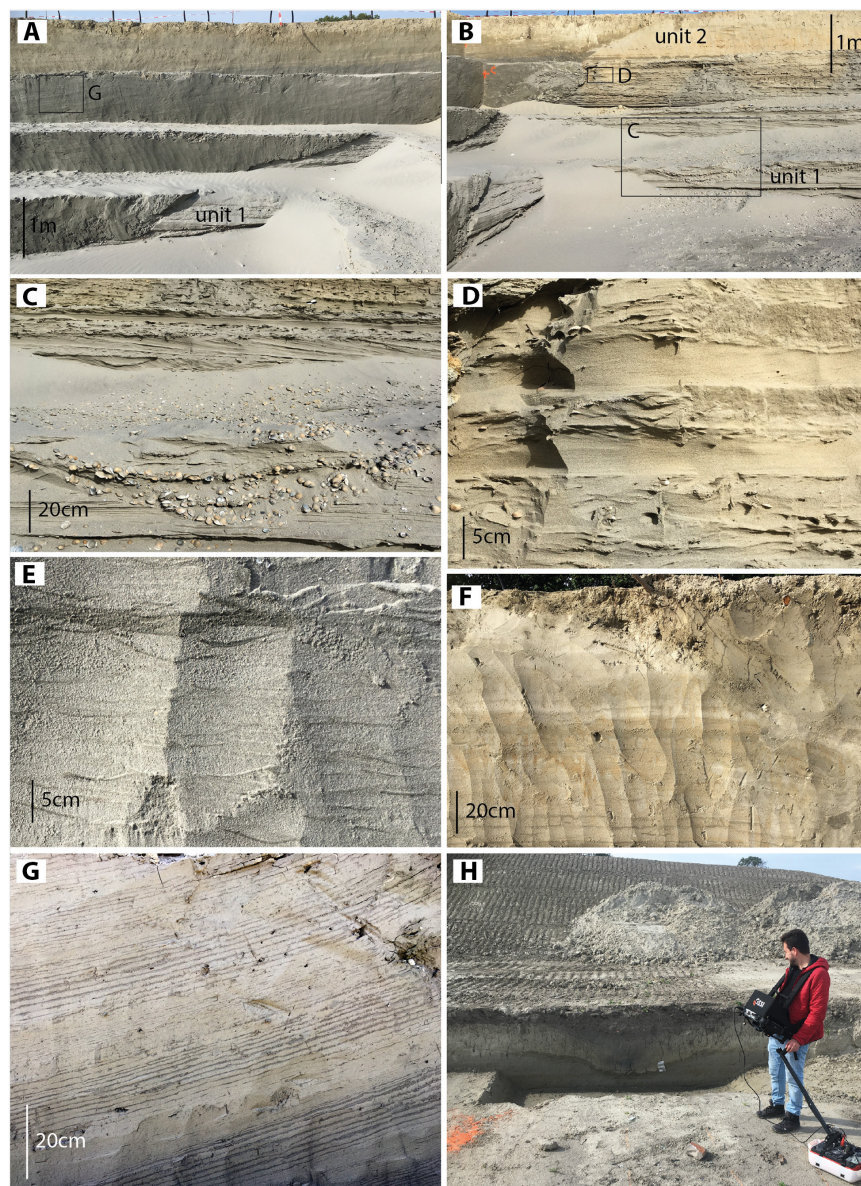


**FIGURE 15** Pictures from an archaeological pit crosscutting the GPR units. See location in [Figure 4A](#). (A) Scoured depression infilled by dominantly mud deposits. (B) Crossbedded grey sands of Unit 1 grading upward to beige sands of Unit 2. (C) Trough crossbeds with *Cerastoderma edule* shell lags in Unit 1. (D) Alternating low-angle and ripple cross-stratification. Dominant current is towards the right (SE). (E) Flaser bedding at the top of Unit 1. (F) Flat-bedded heterolithic stratification (Unit 2), vanishing upward due to ploughing and plant bioturbation. Note the redox front. (G) Tidal rhythmites forming the heterolithic deposits the scour fill. The bundles encompass 12–14 sand-mud couplets. (H) Minor ditch infilled by massive clay incised at the top of Unit 2. Those ditches are the only remnants of medieval dikes.

[Figures 9 and 10](#)). The decrease in channel size and lateral migration from Unit 1 to Unit 2 is consistent with the progressive infilling and reduction of the tidal prism, and correlative decrease in energy and increase in mudiness, as expected in general models of tidal flats and estuarine valley fills (Hugues, 2012; Tessier, 2012). This is consistent with the overall upward and also westward fining of surface sediments as the estuarine river migrated to the west at the same time it shrunk ([Figure 8](#)). Unit 3 corresponds to the silty-clayey facies sampled in core 5 ([Figure 10](#)). The *Scrobicularia* and foraminifera in this facies ([Figure 14D,F](#)) indicate an estuarine (brackish) setting until the end of deposition. Taken together, these results build a coherent picture of an estuarine environment with channels and intertidal flats evolving towards a salt marsh.

The redox front corresponding to the colour transition from grey to beige sand ([Figure 15F](#)) coincides with the shift from the freshwater zone to the saturated and/or saline zone in an area where the groundwater fluctuation is influenced by tides, in addition to its seasonal variation (Burdige, 2011). In the area surrounding the Grand Port Maritime de Dunkerque, the groundwater depth is generally between 1 m and 1.5 m below the soil surface. This depth can vary by a few decimetres depending on meteorological conditions, whether there are wet or dry periods (Cardin et al., 2009). In the study area, a bit further south, the presence of saltwater is confirmed at a depth of 1.75–2.35 m (Lebbe et al., 2018). This matches the transition from red sand to grey sand. Thus, the beige sand would be the unit where phreatic waters could be drained slowly, due to the occurrence of permeability barriers (clay

layers), above a less oxidative, saturated body of saline or brackish water that would keep the grey sand unleached. Redox fronts with gleys in the contact zone between anoxic groundwater and oxic surface water are best developed in old polders, due to drainage restrictions correlative to the presence of an embankment, and thus a longer time for surface water infiltration (Merz et al., 2005).

In this interpretation, the grey to beige sand transition would be diagenetic and not stratigraphic, although Unit 2, closer to the surface, would be generally beige. In the studied pit exposure, the facies succession below the scour depression is fining and thinning upwards, and shows an overall decrease in energy and rate of deposition. This compares with core 4, where upward decrease in sand mode and increase in silt fraction reflects the relative decrease in current velocity and increase in suspension load, a feature typical of the transition from tidal flat to salt marsh sediments (Rahman & Plater, 2014; Wei et al., 2020). This infilling of the accommodation space is consistent with the overall progradation of the Denna tidal flats, correlated to the westward migration of its main channel.

## 5.2 | Effects of land reclamation

The extensive GPR mapping shows an increase in flat strata at the boundary between Unit 2 and Unit 1. Upward flattening of strata is expected to occur from channel bars to tidal flat in the course of lateral accretion and migration of tidal channels. However, in most GPR profiles, the boundary between the two units correspond to a top lap surface (e.g. P2 in Figure 9). This suggests a rather abrupt supply of sediments and increase in accommodation that must be discussed.

Unit 2 could be infilling lows created by peat compaction, as demonstrated in the East Dunkerque area by Mrani-Alaoui (2006), and reviewed by Bartholdy (2012), or peat mining, as demonstrated further west in the French part of the coastal plain (Lançon & Boulén, 2019). However, where peat is present at surface, it is generally also present in the underlying Holocene deposits, and the available boreholes that have traversed the Holocene in the study area show no peat levels (Desoutter, 2020). More probably, the accommodation space of Unit 2 could result from a relatively higher aggradation rate of the last channel belts of Unit 1 (see P2 in Figure 9).

The average sand content of deposits in Unit 2 is high enough for them to be imaged on most of the GPR profiles. This is unexpected in upper tidal flats, the elevation of which might correspond to that of Unit 2, and where normally mud is deposited. At this elevation, in the study area, mud is present only as the infilling of confined channels in Unit 2 or Unit 3, or in the tidalites infilling

scour depressions such as that illustrated in the pit section (Figure 15A,G). The origin of sand in the flat strata of Unit 2 must therefore be questioned.

A first idea is that Unit 2 flat strata could correspond to crevasse splays. This would make sense if the lows infilled by Unit 2 are flanked by meander belts. However, crevasse splays, well-documented in the Rhine-Meuse delta (van Dinter, 2017), are less common in estuaries, except at the fluvial-tidal transition (Boechat Albernaz et al., 2020). Also, (i) no typical levee geometry has been observed in Unit 1 and (ii) Unit 2 flat strata thin towards channels, as opposed to what would be expected in crevasse splays (if the channels were feeders).

The supply of sand in polders may also occur as wash-over deposits, formed when the coastal barrier is breached during storm events. Kilometre-sized sand sheets invaded the back-barrier tidal flat of the Wadden Sea islands (Flemming, 2012) or the Rhine-Meuse area (de Haas et al., 2018) during the medieval periods of lowering of the dune belt. The idea of a surge and rapid deposition of these surface sands is in accordance with the preservation of delicate triactin sponge spicules, which imply that the sediment was not much reworked as would be the case for long-term tidal stirring in the estuarine channels and bars. Sponge spicules have been observed in tidal flats of the Wadden Sea (Bulian et al., 2019), but in a much more open location than that supposed for the Denna estuary by the end of infilling (sponge spicules are found in Unit 3).

The continued supply of sand until after the final infilling of Unit 3 (see P4 in Figure 10) could be partly indebted to aeolian supply to the upper intertidal flats. Significant coastal dune erosion and reworking might have happened after 400 AD (Meurisse-Fort, 2008). To the east of the area, the town of Loon-Plage is located on a fossil dune field corresponding to the western tip of the coastal barrier that closed the Denna estuary to the east. The westward elongation of the barrier may have made this aeolian source an increasing component of the sand finally supplied in the Denna area. The presence of frosted quartz grains in the cores (Figure 14C) supports reworking of quartz grains rounded in an aeolian environment. However, such grains are found also at depth in the cores, and their morphogenesis could be inherited from an older story.

Finally, another explanation for at least some of the flat strata of Unit 2 is to relate them to either controlled flow ingress across locks or non-controlled catastrophic surges across dike breaches. Sheet flows could have invaded the polders following extremely high-water, bringing about dike breaches. This occurred many times during medieval land reclamation in the Netherlands (Vos, 2015). Most of the topographic imprint of the related sand bodies would have been erased by agriculture, especially ploughing. Ploughing is possibly in itself an additional cause for the illuviation of

mud-sized particles and the relative increase in sandiness at surface (Dent et al., 1976). Still, even old polders generally keep the footprint of the grain-size distribution of the tidal flat that was embanked (Jongepier et al., 2015; Missiaen et al., 2017). Thus, in the Denna area, a more careful assessment of the surface grain-size distribution would be necessary to confirm the local heterogeneities observed in surface conductivity maps (Figure 8), and to see whether they follow the natural logic of channel-attached tidal flats, or their embankments and possible overflows.

### 5.3 | Archaeological perspective

Reclamation was realised through dike building, on the open-coast tidal flats of Germany and Denmark (Hadler et al., 2022), and along estuarine rivers of the Netherlands, where they date back to Antiquity (Nieuwhof, 2010). In the French Flemish coastal plain, the intensification of embanking, starting in the 10th and 11th centuries, is correlated with the systematic expansion of human settlements behind the dikes, documented and dated by ceramic materials (Lançon & Boulen, 2019). Diking not only prevented submersions but also limited the return of sediments to the channel whenever they occurred, and therefore accelerated land emergence. Dike breaches were early documented in the medieval archaeology of the Netherlands (Ameryckx, 1953). Breaches created in dikes during stormy episodes associated with high tides would concentrate cascading flows in the polders and generate plunge pools corresponding to the scour depressions later infilled by mud as ponds (Lançon, 2022). Alternatively, the ponds could be fully dug by people and used as freshwater tanks (Deschodt et al., 2021), but in this case their alignment with dikes remains to be explained.

Recent archaeological studies conducted by INRAP shed light on the history of occupation in the estuarine zone of the Denna estuary during the Middle Ages (Lançon, 2017; Lançon, 2022). Radiocarbon datings on *Cerastoderma* found in living position suggest final deposition of Unit 1 by the end of the 6th century. Archaeological objects collected in Unit 1 range from the 5th to the 9th centuries. This marks the end of the natural evolution of the drainage network, before the development of embankments. The Denna channel, navigable at least until the 12th century, gradually closed through reclamation of the tidal flats and back-barrier areas located eastward. Reclamation lasted between the 10th and 15th centuries. Land emergence, characterised by the clay-organic fills of ditches with *Scrobicularia*, typical of Unit 2, became widespread from the 9th century onwards. The dike system progressed stepwise from east to west between Loon-Plage and the Denna, in the 11th, 13th and 15th centuries. In the

study area, at least four dike fronts, spaced about 100 m apart, can be located from historical and archaeological data, west of the pond lines (Figure 11). The orientation of the dikes followed that of the eastern bank of the Denna, which was separated from the dikes by mud flats.

### 5.4 | Tentative geomorphological model of the Denna polders

The geophysical results can be interpreted in the light of archaeological knowledge. The hypothesis that embankment not only matches but also partly controls the transition from Unit 1 to Unit 2 is based on several observations summarised in a sketch (Figure 16). The dikes (generally not preserved) and near-surface channel fills

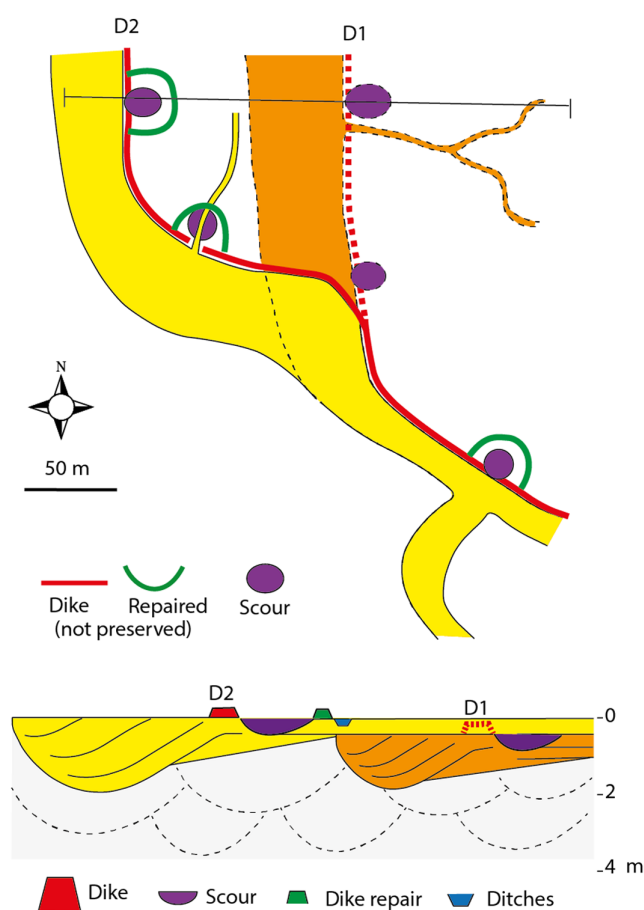


**FIGURE 16** Schematic interpretation of the relationship between the stratigraphic architecture and embankment of the area in the Middle Age. The dikes, associated with ditches, are diachronous from E to W. They control the abrupt decrease of energy of deposition in the polders and may force the active channels to migrate westward. The stepwise shift of the dike front towards the west may coincide with episodes of scour in the lee of breaches formed during submersion events. Such breaches could be repaired by surrounding dikes, some others not.

are commonly aligned. Shallow and narrow channels, present only eastward of the dikes (Figure 11), may have formed as tidal creeks and were possibly reused as ditches to drain out the polders when the dikes were breached. While abrupt terminations of channels mapped in Unit 1 could be the effect of truncation, the network of shallow channels of Unit 2 is more complete and show striking features such as wide channels ending against dikes, or shrinking drastically across dikes (Figure 11). The same relationships have been documented by Jongepier et al. (2015) and Missiaen et al. (2017) on polders of the Scheldt estuary.

The results from the Denna suggest that reclamation followed and possibly forced the westward migration of the main estuarine river channel. The geometry of shallow channel fills supports this latter hypothesis, with abrupt bends (i) towards the west of the main eastern branch of the estuarine river and (ii) towards the north of the Schelfvliet (Figure 8), plus the transition from a meandering to straight course downstream of the latter. These features are consistent with flow deflection towards the west that cannot be a consequence of lateral migration of those channels. This, furthermore, occurs in an area where most archaeological evidence of embankment are found. This tentative reconstruction points to at least two stages of accretion of Unit 2, each associated with the construction of a dike (Figure 16), but there may be as many steps as embankment stages. By the end, the remaining channel of the Denna would be less mobile due to a decrease in tidal prism forced by reclamation (Schrijvershof et al., 2020). This would explain the dominantly clayey infilling of Unit 3 and Unit 2 channels, contrasting with the dominant sandy nature of Unit 2 sheet strata.

Sheet flows could supply sand to the polders, either in a controlled way as transitional polders (Weisscher et al., 2022), or more probably due to catastrophic dike breaches. Probably only dike overflow could form the observed scour depressions. Some breaches could be repaired or surrounded by new dikes, or abandoned at the occasion of new dike building further west (Figure 16). The 4 m deep scour observed in the pit section would have been left connected to the tidal flat seaward of the breach for at least 2 years, based on the number of tidalites preserved in the mud fill (10 cm/neap-spring cycle). The final diversion of the Denna to the west outside the study area may have been caused by an extreme flood associated with a storm event, as documented for the 15th century in the Netherlands (Kleinhans et al., 2010; de Haas et al., 2018). More data west of the study area would be necessary to tell the end of the story, but unfortunately it is also a more clayey area and therefore not appropriate for GPR investigations.

## 6 | CONCLUSIONS

This multidisciplinary study combining surface geophysics, sedimentology and archaeology documents the morphology and sedimentary evolution of a 2 km square sector of agricultural land located on the western Flemish coastal plain, corresponding to the palaeo-estuary of the Denna, west of Dunkerque. Over 30 km of GPR profiles, correlated with vibrocores and observations in archaeological pits, could be compared with extensive mapping of surface conductivity. The results can be summarised as follows:

1. At the large scale, the conductivity map shows a surface hydrographic network consisting of a sinuous to meandering network of anastomosed channels infilled with muddy sediments. This corresponds to the final stage of estuarine deposition. Mud-filled enclosed depressions are also detected on the conductivity map, which are interpreted as the infill of breaches caused by catastrophic submersion of medieval dikes.
2. Two stratigraphic units are revealed by GPR data. The upper one is formed by 0.5–1 m thick aggrading sand layers traversed by muddy channel fills matching the pattern of the conductivity map. Some of these channels were reworked into ditches during reclamation. The lower unit, over 4 m in thickness, is an overall aggrading deposit of 1–2 m thick meander bars.
3. Vibrocores show that both units are predominantly composed of fine sand, containing marine-derived bioclasts (including delicate triactin sponge spicules), as well as foraminifera typical of estuarine environments, and a minor fraction of aeolian quartz. The infill of the last channels is dominated by silt. Below the ploughed ground, the sediments are oxidised down to the phreatic water level.
4. Exposures of these deposits in an archaeological pit provide facies details indicating that (i) the lower unit is composed of compound crossbeds thinning and fining upwards to heterolithic tidal flat deposits and (ii) mud-filled enclosed depressions have a scoured bottom and are infilled by tidal rhythmites; based on the number of these, the breach in the dike is thought to have remained open for about 2 years.

These results highlight some new elements regarding sedimentary dynamics and stratigraphy in reclaimed areas of the Flemish coastal plain. Radiocarbon dating of shells and archaeological artefacts collected indicate that the transition from the lower to upper unit began in the 7th century, during the period of the very first embankments. The upper unit could be partly the result of ingression of sheet flows inside the polders across breaches

formed during extremely high-water levels. This would explain the abnormally high sandiness of the upper part of the infill.

## ACKNOWLEDGEMENTS

This work, part of Rachid Ouchaoou PhD thesis, has benefitted from funding from SFR Campus de la Mer, and is indebted to INRAP for accessing to works in progress and geoarchaeological data. The authors would like to thank the guest editor, Sergio Longhitano, for the opportunity of publishing it in this special issue. Maarten Kleinhans and an anonymous reviewer are warmly thanked for their constructive reviews.

## DATA AVAILABILITY STATEMENT

The GPR data presented in this work are part of a larger database that can be shared upon reasonable request to the corresponding author.

## ORCID

Jean-Yves Reynaud  <https://orcid.org/0000-0003-3665-8149>

## REFERENCES

- Ameryckx, J.B. (1953) Het ontstaan en evolutie van het Zwin in België. *Natuurwetenschappelijk Tijdschrift*, 34(4–5), 99–110.
- Armynot du Châtelet, E., Duvaut-Robine, A. & Meurisse-Fort, M. (2019) Caractérisation par les foraminifères des environnements archéologiques et du cadre paysager – exemple d'application sur Quentovic (embouchure de la Canche, France). *Quaternaire*, 30, 211–223. <https://doi.org/10.4000/quaternaire.11794>
- Bakker, J.P., Berg, M.P., Grootjans, A.P., Olf, H., Schrama, M., Reijers, V.C. & Van der Heide, T. (2023) Biogeomorphological aspects of a model barrier Island and its surroundings—interactions between abiotic conditions and biota shaping the tidal and terrestrial landscape: a synthesis. *Ocean and Coastal Management*, 239, 106624. doi:10.1016/j.ocecoaman.2023.106624
- Baeteman, C. & Declerck, P.-Y. (2002) A synthesis of early and middle Holocene coastal changes in the Western Belgian lowlands. *Belgeo*, 2, 77–107.
- Baeteman, C. (2007) Roman peat-extraction pits as possible evidence for the timing of coastal changes: an example from the Belgian coastal plain. In: Beenakker, J.J., Horsten, F.H., De Kraker, M.J. & Renes, H. (Eds.) *Landschap in ruimteentijd*. Amsterdam: Aksant, pp. 16–25.
- Baeteman, C. (2018) The Coastal Plain of Belgium, joint product of natural processes and human activities. In: Demoulin, A. (Ed.) *Landscapes and landforms of Belgium and Luxembourg*. Cham: Springer International Publishing, pp. 313–334. doi:10.1007/978-3-319-58239-9\_19
- Bartholdy, J. (2012) Salt marsh sedimentation. In: Davis, R., Jr. & Dalrymple, R. (Eds.) *Principles of tidal sedimentology*. Dordrecht: Springer, pp. 151–185. doi:10.1007/978-94-007-0123-6\_8
- Boechat Albernaz, M., Roelofs, L., Pierik, H.J. & Kleinhans, M.G. (2020) Natural levee evolution in vegetated fluvial-tidal environments. *Earth Surface Processes and Landforms*, 45(15), 3824–3841. doi:10.1002/esp.5003
- Bristow, C. & Jol, H. (2003) An introduction to ground penetrating radar (GPR) in sediments. *Geological Society of London, Special Publication*, 211, 1–7. <https://doi.org/10.1144/GSL.SP.2001.211.01.01>
- Bulian, F., Enters, D., Schlütz, F., Scheder, J., Blume, K., Zolitschka, B. & Bittmann, F. (2019) Multi-proxy reconstruction of Holocene palaeoenvironments from a sediment core retrieved from the Wadden Sea near Norderney, East Frisia, Germany. *Estuarine, Coastal and Shelf Science*, 225, 106251. <https://doi.org/10.1016/j.ecss.2019.106251>
- Burdige, D.J. (2011) *Estuarine and coastal sediments – coupled biogeochemical cycling*. Treatise on Estuarine and Coastal Science. Waltham: Academic Press. <https://doi.org/10.1016/B978-0-12-374711-2.00511-8>
- Cardin, C., Joublin, F., Dufrenoy, R. & Braibant, G. (2009) Grand Port Maritime de Dunkerque: inventaire et diagnostic du réseau. Prélèvement et piézométrie. Octobre 2009. BRGM/RP-58014-FR.
- Choi, K.S., Hong, C.M., Kim, M.H., Oh, C.R. & Jung, J.H. (2013) Morphologic evolution of macrotidal estuarine channels in Gomso Bay, west coast of Korea: implications for the architectural development of inclined heterolithic stratification. *Marine Geology*, 346, 343–354. doi:10.1016/j.margeo.2013.10.005
- Clarke, M.L. & Rendell, H.M. (2009) The impact of North Atlantic storminess on western European coasts: a review. *Quaternary International*, 195, 31–41. doi:10.1016/j.quaint.2008.02.007
- Dalrymple, R.W. (1992) Tidal depositional systems. In: Walker, R.G. & James, N.P. (Eds.) *Facies models*. Toronto: Geological Association of Canada, pp. 195–218.
- Dent, D.L., Downing, E.J.B. & Rogaar, H. (1976) Changes in the structure of marsh soils following drainage and arable cultivation. *Journal of Soil Science*, 27, 250–265. doi:10.1111/j.1365-2389.1976.tb01995.x
- Deschodt, L., Lançon, M., Desoutter, S., Hulin, G., Simon, F.-X., Vanwaslscappel, B., Créteur, Y., Broes, F., Devred, V., Favier, D. & Le Bayon, A.-L. (2021) Exploration archéologique de 170 hectares de plaine maritime (Bourbourg, Saint-Georges-sur-l'Aa, Craywick, Nord de la France): restitution de la fermeture d'un estuaire au Moyen Âge et mise en évidence de mares endiguées. *Bulletin de la Société Géologique de France*, 192(1), 12. doi:10.1051/bsgf/2021004
- Desoutter, S. (2018) Bourbourg, Saint-Georges-sur-l'Aa, Craywick. Rapport de diagnostic. Inrap Hauts-de-France, Gisly, 3 vol.
- Desoutter, S. (2019) Gravelines, Loon-Plage. Rapport de diagnostic. Inrap Hauts-de-France, Gisly, 3 vol.
- Desoutter, S. (2020) Gravelines, Loon-Plage. Rapport de diagnostic. Inrap Hauts-de-France, Gisly, 3 vol.
- van Dinter, M. (2017) Living along the Limes: landscape and settlement in the Lower Rhine Delta during Roman and Early Medieval times. PhD Utrecht University, Faculty of Geosciences, Department of Physical Geography, Utrecht. Utrecht Studies. *Geosciences*, 135, 223.
- Doolittle, J.A. & Brevik, E.C. (2014) The use of electromagnetic induction techniques in soils studies. *Geoderma*, 223–225, 33–45. doi:10.1016/j.geoderma.2014.01.027

- Donselaar, M.E. & Geel, C.R. (2007) Facies architecture of heterolithic tidal deposits: the Holocene Holland tidal basin. *Netherlands Journal of Geosciences*, 86(4), 389–402. <https://doi.org/10.1017/S001677460002360X>
- Dubois, G. (1924) Recherches sur les terrains quaternaires du Nord de la France. *Mémoires de la Société Géologique du Nord*, VIII(I), 356.
- Ducrocq, E., Vannoye, S. & Mazouni, F. (2022) La recharge artificielle de la nappe pour pérenniser la ressource: retour d'expérience de l'unité de Moulle (Pas-de-Calais). *TSM*, 12, 43–52. <https://doi.org/10.36904/202212043>
- Dynesius, M. & Nilsson, C. (1994) Fragmentation and flow regulation of river systems in the northern third of the world. *Science*, 266(5186), 753–762. <https://doi.org/10.1126/science.266.5186.753>
- Flemming, B.W. (2012) Siliciclastic Back-Barrier Tidal Flats. In: Davis, R.A. & Dalrymple, R.W. (Eds.) *Principles of tidal sedimentology*. Dordrecht: Springer, pp. 231–267. [https://doi.org/10.1007/978-94-007-0123-6\\_10](https://doi.org/10.1007/978-94-007-0123-6_10)
- Gong, W., Schuttelaars, H. & Zhang, H. (2016) Tidal asymmetry in a funnel-shaped estuary with mixed semidiurnal tides. *Ocean Dynamics*, 66, 637–658. <https://doi.org/10.1007/s10236-016-0943-1>
- de Haas, T., Pierik, H.J., van der Spek, A.J.F., Cohen, K.M., van Maanen, B. & Kleinhans, M.G. (2018) Holocene evolution of tidal systems in The Netherlands: effects of rivers, coastal boundary conditions, eco-engineering species, inherited relief and human interference. *Earth-Science Reviews*, 177, 139–163. <https://doi.org/10.1016/j.earscirev.2017.10.006>
- Hadler, H., Wilken, D., Bäuml, S., Fischer, P., Rabbel, W., Willershäuser, T., Wunderlich, T. & Vöt, A. (2022) The Trendermarsch polder (North Frisia, Germany)—geophysical and geoarchaeological investigations of an anthropogenic medieval coastal landscape and its vulnerability against natural hazards. *Geomorphology*, 418, 108461. <https://doi.org/10.1016/j.geomorph.2022.108461>
- Hauser, S.J. (2020) Long live the heritage of petroleum—discoveries of former oil sites in the Port City of Dunkirk. *Urban Science*, 4, 22.
- Herrera-García, G., Ezquerro, P., Tomás, R., Béjar-Pizarro, M., López-Vinielles, J., Rossi, M., Mateos, R.M., Carreón-Freyre, D., Lambert, J., Teatini, P., Cabral-Cano, E., Erken, G., Galloway, D., Hung, W.-C., Kakar, N., Sneed, M., Tosi, L. & Wang, H. (2021) Mapping the global threat of land subsidence. *Science*, 371, 34–36. <https://doi.org/10.1126/science.abb8549>
- Hijma, M.P., Cohen, K.M., Hoffmann, G., der Spek, A.J.F.V. & Stouthamer, E. (2009) From river valley to estuary: the evolution of the Rhine mouth in the early to middle Holocene (western Netherlands, Rhine-Meuse delta). *Netherlands Journal of Geosciences*, 88, 13–53. <https://doi.org/10.1017/S0016774600000986>
- Hoeksema, R.J. (2007) Three stages in the history of land reclamation in The Netherlands. *Irrigation and Drainage*, 56, S113–S126. <https://doi.org/10.1002/ird.340>
- Hughes, Z.J. (2012) Tidal channels on tidal flats and marshes. In: Davis, R.A. & Dalrymple, R.W. (Eds.) *Principles of tidal sedimentology*. Dordrecht: Springer, pp. 269–300. [https://doi.org/10.1007/978-94-007-0123-6\\_11](https://doi.org/10.1007/978-94-007-0123-6_11)
- IFREMER. (1986) Le Littoral de la Région Nord-Pas de Calais qualité du milieu marin. *Rapports Scientifiques Et Techniques De L'Ifremer. Convention de Coopération Région Nord - Pas de Calais*, 3, 136.
- Jongepier, I., Wang, C., Missiaen, T., Soens, T. & Temmerman, S. (2015) Intertidal landscape response time to dike breaching and stepwise re-embankment: a combined historical and geomorphological study. *Geomorphology*, 236, 64–78. <https://doi.org/10.1016/j.geomorph.2015.02.012>
- Kleinhans, M.G., Weerts, H.J.T. & Cohen, K.M. (2010) Avulsion in action: reconstruction and modelling sedimentation pace and upstream flood water levels following a medieval tidal-river diversion catastrophe (Biesbosch, The Netherlands, 1421–1750 AD). *Geomorphology*, 118(1–2), 65–79. <https://doi.org/10.1016/j.geomorph.2009.12.009>
- Koster, K., Stafleu, J., Vos, P.C. & van der Meulen, M.J. (2020) Can we elevate the subsiding coastal plain of The Netherlands with controlled sedimentation? *Proceedings of the International Association of Hydrological Sciences*, 382, 767–773. <https://doi.org/10.5194/piahs-382-767-2020>
- de Kraker, A.M.J. (2015) Flooding in river mouths: human caused or natural events? Five centuries of flooding events in the SW Netherlands, 1500–2000. *Hydrology and Earth System Sciences*, 19, 2673–2684. <https://doi.org/10.5194/hess-19-2673-2015>
- Krinsley, D. & Trusty, P. (1985) Environmental interpretation of quartz grain surface textures. In: Zuffa, G.G. (Ed.) *Provenance of arenites*. Dordrecht: Springer Netherlands, pp. 213–229. [https://doi.org/10.1007/978-94-017-2809-6\\_10](https://doi.org/10.1007/978-94-017-2809-6_10)
- Kvale, E.P., Archer, A.W. & Johnson, H.R. (1989) Daily, monthly, and yearly tidal cycles within laminated siltstones of the Mansfield Formation (Pennsylvanian) of Indiana. *Geology*, 17, 365–368. [https://doi.org/10.1130/0091-7613\(1989\)017<0365:DMAYTC>2.3.CO;2](https://doi.org/10.1130/0091-7613(1989)017<0365:DMAYTC>2.3.CO;2)
- Lambeck, K., Esat, T.M. & Potter, E.-K. (2002) Links between climate and sea levels for the past three million years. *Nature*, 419, 199–206. <https://doi.org/10.1038/nature01089>
- Lançon, M. (2022) Craywick, St-Georges-sur-Aa, Gravelines-Loon-Plage. Rapport de diagnostic. Inrap Hauts-de-France, Gislis, 3 vol.
- Lançon, M. (2017) Rapport de diagnostic: Bourbourg, Saint-Georges-sur-l'Aa, Le Grand Palynck Dyck, Port autonome de Dunkerque. INRAP HdF.
- Lançon, M. & Boulen, M. (2019) Les occupations humaines de la plaine maritime flamande à l'Holocène supérieur. Un changement de paradigme? *Quaternaire*, 30(4), 311–334. <https://doi.org/10.1051/bsgf/2021004>
- Lebbe, L., Depret, D., Claus, J. & Devriese, G.J. (2018) Salt water intrusion in the breakthrough valley of the river Aa between the Flemish coastal plain and the Saint Omer basin (France). In E3S Web of Conferences, EDP Sciences. <https://doi.org/10.1051/e3sconf/20185400017>
- Malham, S.K., Hutchinson, T.H. & Longshaw, M. (2012) A review of the biology of European cockles (*Cerastoderma* spp.). *Journal of the Marine Biological Association of the United Kingdom*, 92(7), 1563–1577. <https://doi.org/10.1017/S0025315412000355>
- Makaske, B. & Weerts, H.J. (2005) Muddy lateral accretion and low stream power in a sub-recent confined channel belt, Rhine-Meuse delta, central Netherlands. *Sedimentology*, 52(3), 651–668. <https://doi.org/10.1111/j.1365-3091.2005.00713.x>

- Margotta, J. (2014) Stratigraphic architecture and sedimentary evolution of the Holocene deposits in the French Flemish coastal plain, Northern France. Unpublished PhD thesis, U-Lille 1 <https://www.theses.fr/2014LIL10012>
- Margotta, J., Trentesaux, A. & Tribouvillard, N. (2016) Tidally-modulated infilling of a large coastal plain during the Holocene; the case of the French Flemish Coastal plain. In: Tessier, B. & Reynaud, J.Y. (Eds.) *Contributions to Modern and Ancient Tidal Sedimentology: Proceedings of the Tidalites 2012 Conference*. Chichester: John Wiley and Sons, Ltd., pp. 243–260. <https://doi.org/10.1002/9781119218395.ch14>
- Mastrocicco, M. & Colombani, N. (2021) The issue of groundwater salinization in coastal areas of the Mediterranean region: a review. *Water*, 13, 90. <https://doi.org/10.3390/w13010090>
- Mathys, M. (2009) The Quaternary geological evolution of the Belgian Continental Shelf, southern North Sea. Unpublished PhD thesis, Ghent University, Ghent, 371 p <https://biblio.ugent.be/publication/716421>
- McMichael, C., Dasgupta, S., Ayeb-Karlsson, S. & Kelman, I. (2020) A review of estimating population exposure to sea-level rise and the relevance for migration. *Environmental Research Letters*, 15, 123005. <https://doi.org/10.1088/1748-9326/abb398>
- Merz, C., Schuhmacher, P., Winkler, A. & Pekdeger, A. (2005) Identification and regional quantification of hydrochemical processes at the contact zone between anoxic groundwater and surface water in poldered floodplains (Oderbruch polder, Germany). *Applied Geochemistry*, 20, 241–254. <https://doi.org/10.1016/j.apgeochem.2004.09.005>
- Meurisse-Fort, M. (2008) Enregistrement haute résolution des massifs dunaires: Manche, mer du Nord et Atlantique: le rôle des tempêtes. Ed. Publibook and Unpublished PhD thesis, U-Lille 1, 350 p.
- Missiaen, T., Jongepier, I., Heirman, K., Soens, T., Gelorini, V., Verniers, J., Verhegge, J. & Crombé, P. (2017) Holocene landscape evolution of an estuarine wetland in relation to its human occupation and exploitation: Waasland Scheldt polders, northern Belgium. *Netherlands Journal of Geosciences*, 96, 35–62. <https://doi.org/10.1017/njg.2016.24>
- Mrani-Alaoui, M. (2006) Evolution des environnements sédimentaires holocènes de la plaine maritime flamande du Nord de la France: eustatisme et processus. Unp. PhD thesis, Université du Littoral, Côte d'Opale, Dunkerque, 211 p.
- Nienhuis, J.H., Ashton, A.D., Edmonds, D.A., Hoitink, A.J.F., Kettner, A.J., Rowland, J.C. & Törnqvist, T.E. (2020) Global-scale human impact on delta morphology has led to net land area gain. *Nature*, 577, 514–518. <https://doi.org/10.1038/s41586-019-1905-9>
- Nieuwhof, A. (2010) Living in a dynamic landscape: prehistoric and proto-historic occupation of the northern-Netherlands coastal area. In: Marencic, H., Eskildsen, K., Farke, H. & Hedtkamp, S. (Eds.) *Science for Nature Conservation and Management: the Wadden Sea Ecosystem and EU Directives*. Proceedings of the 12th International Scientific Wadden Sea Symposium in Wilhelmshaven, Germany, 30 March–3 April 2009. Wadden Sea Ecosystem; No. 26, Common Wadden Sea Secretariat. Groningen: University of Groningen, pp. 174–178.
- Nieuwhof, A., Bakker, M., Knol, E., de Langen, G.J., Nicolay, J.A.W., Postma, D., Schepers, M., Varwijk, T.W. & Vos, P.C. (2019) Adapting to the sea: human habitation in the coastal area of the northern Netherlands before medieval dike building. *Ocean and Coastal Management*, 173, 77–89. <https://doi.org/10.1016/j.ocecoaman.2019.02.014>
- Pauw, P., de Louw, P.G.B. & Essink, G.H.P.O. (2012) Groundwater salinisation in the Wadden Sea area of The Netherlands: quantifying the effects of climate change, sea-level rise and anthropogenic interferences. *Netherlands Journal of Geosciences*, 91, 373–383. <https://doi.org/10.1017/S0016774600000500>
- Peteiro, L.G., Woodin, S.A., Wethey, D.S., Costas-Costas, D., Martínez-Casal, A., Olabarria, C. & Vázquez, E. (2018) Responses to salinity stress in bivalves: evidence of ontogenetic changes in energetic physiology on *Cerastoderma edule*. *Scientific Reports*, 8, 8329. <https://doi.org/10.1038/s41598-018-26706-9>
- Rahman, R. & Plater, A.J. (2014) Particle-size evidence of estuary evolution: a rapid and diagnostic tool for determining the nature of recent saltmarsh accretion. *Geomorphology*, 213, 139–152. <https://doi.org/10.1016/j.geomorph.2014.01.004>
- Reed, D.J., Davidson-Arnott, R. & Perillo, G.M.E. (2009) *Estuaries, coastal marshes, tidal flats and coastal dunes*. Cambridge: University Press, pp. 130–157.
- Reineck, H.F. & Wunderlich, F. (1968) (1968) Classification and Origin of Flaser and Lenticular Bedding. *Sedimentology*, 11, 99–104. <https://doi.org/10.1111/j.1365-3091.1968.tb00843.x>
- Roep, T.B. (1991) Neap-spring cycles in a subrecent tidal channel fill (3665 BP) at Schoorldam, NW Netherlands. *Sedimentary Geology*, 71, 213–230. [https://doi.org/10.1016/0037-0738\(91\)90103-K](https://doi.org/10.1016/0037-0738(91)90103-K)
- Ruz, M.-H., Héquette, A. & Maspataud, A. (2009) Identifying forcing conditions responsible for foredune erosion on the northern coast of France. *Journal of Coastal Research*, 56, 356–360.
- Schrijvershof, R., Van Maren, B., Vermeulen, B. & Hoitink, T. (2020) Intertidal floodplain controls on centennial-scale morphological channel development, EP015-07. <https://ui.adsabs.harvard.edu/abs/2020AGUFMEP015.07S>
- Smith, D.G., De Boer, P.L., Van Gelder, A. & Nio, S.D. (1988) Modern point bar deposits analogous to the Athabasca oil sands, Alberta, Canada. In: de Boer, P.L., Van Gelder, A. & Nio, S.D. (Eds.) *Tide-influenced sedimentary environments and facies*. Dordrecht: Reidel, pp. 417–432.
- Sommé, J., Antoine, P., Cunat-Bogé, N., Lefèvre, D. & Munaut, A.-V. (1999) Le Pléistocène moyen marin de la mer du Nord en France: falaise de Sangatte et formation d'Herzelee [The marine middle Pleistocene of the North Sea in France: Sangatte cliff and Herzelee formation]. *Quaternaire*, 10, 151–160. <https://doi.org/10.3406/quate.1999.1638>
- Sommé, J., Cunat-Bogé, N., Vanhoorne, R. & Wouters, K. (2004) La Formation de Loon: les dépôts pléistocènes marins profonds de la plaine maritime du Nord de la France. *Quaternaire*, 15(4), 319–327. [https://www.persee.fr/doc/quate\\_1142-2904\\_2004\\_num\\_15\\_4\\_1778](https://www.persee.fr/doc/quate_1142-2904_2004_num_15_4_1778)
- Ters, M. (1973) Les variations du niveau marin depuis 10000 ans, le long du littoral atlantique français. Actes du colloque: 9e Congrès international de l'INQUA: Le Quaternaire Géodynamique, stratigraphie et environnement. INQUA, 114-136.
- Tessier, B. (1993) Upper intertidal rhythmites in the Mont-Saint-Michel Bay (NW France): perspectives for palaeoreconstruction. *Marine Geology*, 110, 355–367. [https://doi.org/10.1016/0025-3227\(93\)90093-B](https://doi.org/10.1016/0025-3227(93)90093-B)
- Tessier, B. (2012) Stratigraphy of tide-dominated estuaries. In: Davis, R.A. & Dalrymple, R.W. (Eds.) *Principles of Tidal Sedimentology*.

- Cham: Springer Nature, pp. 109–128. [https://doi.org/10.1007/978-94-007-0123-6\\_6](https://doi.org/10.1007/978-94-007-0123-6_6)
- Thomas, R.G., Smith, D.G., Wood, J.M., Visser, J., Calverley-Range, E.A. & Koster, E.H. (1987) Inclined heterolithic stratification—Terminology, description, interpretation and significance. *Sedimentary Geology*, 53, 123–179. [https://doi.org/10.1016/S0037-0738\(87\)80006-4](https://doi.org/10.1016/S0037-0738(87)80006-4)
- Ulbrich, U., Christoph, M., Pinto, J.G. & Corte-Real, J. (2019) Dependence of winter precipitation over Portugal on NAO and Baroclinic Wave Activity. *International Journal of Climatology*, 19, 379–390, 1999. [https://doi.org/10.1002/\(SICI\)1097-0088\(19990330\)19:4<379::AID-JOC357>3.0.CO;2-8](https://doi.org/10.1002/(SICI)1097-0088(19990330)19:4<379::AID-JOC357>3.0.CO;2-8)
- Verhulst, A. & Gottschalk, M.K.E. (Eds.). (1980) Transgressies en occupatie geschiedenis in de kustgebieden van Nederland en België. *Centre belge d'histoire rurale, publication*, 66, 332.
- Vos, P. (2015) *Origin of the Dutch coastal landscape: long-term landscape evolution of the Netherlands during the Holocene, described and visualized in national, regional and local palaeogeographical map series* [PhD]. Groningen: Barkhuis, 359 pp.
- Wanner, H., Beer, J., Bütikofer, J., Crowley, T.J., Cubasch, U., Flückiger, J., Goosse, H., Grosjean, M., Joos, F., Kaplan, J.O., Küttel, M., Müller, S.A., Prentice, I.C., Solomina, O., Stocker, T.F., Tarasov, P., Wagner, M. & Widmann, M. (2008) Mid-to Late Holocene climate change: an overview. *Quaternary Science Reviews*, 27, 1791–1828. <https://doi.org/10.1016/j.quascirev.2008.06.013>
- Wei, W., Dai, Z., Pang, W., Wang, J. & Gao, S. (2020) Sedimentary zonation shift of tidal flats in a meso-tidal estuary. *Sedimentary Geology*, 407, 105749. <https://doi.org/10.1016/j.sedgeo.2020.105749>
- Weisscher, S.A.H., Baar, A.W., van Belzen, J., Bouma, T.J. & Kleinhans, M.G. (2022) Transitional polders along estuaries: driving land-level rise and reducing flood propagation. *Nature-Based Solutions*, 2, 100022. <https://doi.org/10.1016/j.nbsj.2022.100022>
- Wilken, D., Hadler, H., Wunderlich, T., Majchczack, B., Schwardt, M., Fediuk, A., Fischer, P., Willershäuser, T., Klooss, S., Vött, A. & Rabbel, W. (2022) Lost in the North Sea—geophysical and geoarchaeological prospection of the Rungholt medieval dyke system (North Frisia, Germany). *PLoS ONE*, 17(4), e0265463. <https://doi.org/10.1371/journal.pone.0265463>
- de Winter, R.C. & Ruessink, B.G. (2017) Sensitivity analysis of climate change impacts on dune erosion: case study for the Dutch Holland coast. *Climatic Change*, 141, 685–701. <https://doi.org/10.1007/s10584-017-1922-3>

**How to cite this article:** Ouchaou, R., Reynaud, J.-Y., Besse, Y., Tileghouatine, A., Armynot du Châtelet, E., Trentesaux, A. et al. (2024) The depositional record of the French Flemish Coastal plain since antiquity: Impacts of land reclamation in a tide-dominated estuary. *The Depositional Record*, 00, 1–23. Available from: <https://doi.org/10.1002/dep2.279>